Carbon Pricing and Monetary Policy in an Estimated Macro-Climate Model*

Link to most recent version

Sofia Semik†

October 17, 2025

Abstract

I develop and estimate a two-agent New Keynesian (TANK) macro-climate model with energy to study the effects of carbon price shocks on the euro area economy. Using EU ETS data, I document three features of such shocks: a gradual decline in emissions, a temporary surge in inflation, and a contraction in economic activity. The model captures these dynamics through adjustment costs in fossil energy use, limited substitutability between fossil and green energy, and strong complementarities between energy and other inputs. Hand-to-mouth households play an important role, as they are particularly vulnerable to higher energy prices. The estimated model suggests that optimal monetary policy prioritizes output stabilization at the cost of temporarily higher inflation in response to the shock. In the absence of these key frictions, however, the model would prescribe an initially contractionary policy response. A Taylor rule targeting core rather than headline inflation mitigates GDP losses and approximates the welfare-optimal response.

JEL Codes: E52, H23, Q43, Q58
Keywords: Carbon pricing, optimal monetary policy, Bayesian estimation

*I'm grateful for the comments and suggestions I received from colleagues, the participants of the ECB Conference on Monetary Policy 2025, the 2nd International Conference on the Climate-Macro-Finance Interface and the EEA 2025 Annual Congress, and especially for the continuous feedback and support I received from my supervisor Mathias Trabandt. I am very grateful for the hospitality and guidance of Diego Känzig at Northwestern University, where parts of this paper were written during a research visit in the fall of 2024.

†Goethe University Frankfurt am Main, Email: sofia.semik@gmail.com, Web: sofiasemik.com

1 Introduction

As climate change becomes an increasingly pressing global challenge, governments are implementing ambitious policies to accelerate the transition to a low-carbon economy, most notably through carbon pricing. In response, a growing literature has emerged that incorporates environmental dynamics into DSGE frameworks to study the macroeconomic implications of such policies (see for instance Annicchiarico and Di Dio (2015), Diluiso et al. (2021), Coenen et al. (2024), Sahuc et al. (2025)). However, substantial uncertainty remains about how carbon price increases affect key macroeconomic variables, especially in the context of rising concerns about "greenflation" — the inflationary pressure stemming from higher energy costs (Schnabel, 2022). To effectively design and evaluate monetary policy responses to macroeconomic dynamics caused by carbon policy initiatives, it is crucial to develop models that closely align with the empirical responses to carbon pricing.

In this paper, I develop and estimate a two-agent New Keynesian macro-climate model with energy that accounts for macroeconomic effects of carbon price increases in the euro area observed in the data. I assess the macroeconomic impact of carbon price increases on the EU Emission Trading System (EU ETS) carbon market using local projections. For this I use the carbon price shock series constructed by Känzig (2023), which identifies unexpected changes in ETS emission allowance future prices. My findings suggest that carbon price shocks effectively reduce GHG emissions, though the reduction is not immediate. Instead, emissions decline gradually, likely due to technological constraints and infrastructure limitations that prevent an instantaneous shift away from fossil energy. However, the emission reduction comes at an economic cost for the euro area. The carbon price shock triggers a sharp increase in energy prices, which is then passed on to consumer prices, leading to an immediate rise in headline inflation. Higher energy costs raise production expenses for firms and increase households' energy bills, causing a decline in economic activity. The fall in wages, stemming from firms' higher energy-related costs, further reduces household income, amplifying the drop in consumption and aggregate demand. This downturn is potentially exacerbated by monetary policy tightening, as central banks respond to inflationary pressures by raising interest rates.

To accurately capture these empirical dynamics, I estimate my model using Bayesian impulse response matching. This methodology involves minimizing the distance between the dynamic responses of my model to a carbon price shock and analog objects in the data obtained from the local projections. My model accounts well for the key features of the estimated impulse response functions: a gradual decline in emissions, an immediate surge in headline inflation and a significant drop in economic activity. The following parameter specifications are key features for the success of the model fit:

The first non-standard feature of my model is the introduction of quadratic adjust-

ment costs for fossil energy producers, preventing an immediate reduction in fossil energy use following a carbon price shock. The posterior mode of the adjustment cost parameter suggests that these costs are significantly positive. These frictions reflect real-world technological constraints and infrastructure limitations, ensuring that the delayed decline in emissions observed in the data is replicated in the model. Second, the estimated elasticity of substitution between green and fossil energy is below unity in my model, indicating that these energy sources are complements rather than substitutes. The low substitutability in response to temporary shocks in my model is essential to capturing the strong pass-through from fossil energy prices to aggregate energy prices. Higher substitutability would imply a weaker inflationary response, leading to an underestimation of the observed rise in consumer prices and the associated decline in aggregate demand. Third, there is very strong complementarity of energy in production and consumption. The model assumes that energy is a crucial input for both firms and households, making it difficult to substitute away from energy consumption. This amplifies the economic effects of carbon price shocks, as it makes households and firms more vulnerable to higher energy prices following carbon price shocks. Finally, including hand-to-mouth households into the model helps explaining the significant drop in consumption observed in the data, because they are more vulnerable to energy price increases.

To conduct meaningful policy analysis, it is crucial to use a model that captures the macroeconomic transmission of carbon price shocks. I analyze the role of monetary policy in mitigating the economic costs of such shocks. I compare the implications of a welfare-maximizing Ramsey policy with alternative interest rate rules in response to a carbon price shock. The results highlight a key trade-off for monetary policy: stabilizing inflation would require higher interest rates, but this would amplify the contraction in aggregate demand. The Ramsey planner instead places greater weight on stabilizing real activity, lowering interest rates and accepting temporarily higher inflation to cushion the decline in demand. In contrast, a model without the key features described above, such as limited substitutability in energy use and adjustment costs in fossil energy, implies that optimal monetary policy should be contractionary in response to a carbon price shock, as inflation dynamics dominate and the output response becomes less pronounced.

A Taylor rule that stabilizes core instead of headline inflation comes closer to the optimal monetary policy response. By focusing on core inflation, the central bank effectively "looks through" the temporary surge in energy inflation, avoiding excessive monetary tightening and thus mitigating the fall in demand. While this approach leads to a somewhat larger initial increase in headline inflation, this effect is small and not persistent. In contrast, the mitigation of GDP losses is substantial, making core inflation targeting a welfare-improving policy choice.

This paper contributes to the growing macro-climate DSGE literature by providing an empirically grounded framework for evaluating the macroeconomic effects of carbon

pricing in the euro area. The findings are particularly relevant for the design of monetary policy in the face of inflationary pressures and output losses arising from climate policy initiatives.

Related Literature. This papers contributes to both empirical and theoretical literature on the macroeconomic effects of climate change mitigation policies and potential implications for monetary policy. First, my paper is related to a growing strand of empirical literature assessing the macroeconomic effects of carbon price increases. The empirical part is closely related to Känzig (2023). Känzig uses high-frequency identification of regulatory events on the European carbon market to construct a carbon policy surprise shock series and study the effects on the euro area economy and on emissions. His findings suggest that an increase in the EU ETS carbon price is effective in reducing emissions, but entails economic costs as it creates inflationary pressures and a fall in employment and real activity. Metcalf and Stock (2023) analyze the macroeconomic implications of European carbon taxes. Interestingly, they find that while carbon taxes reduce emissions, they do not lead to a significant reduction in GDP. Similarly, Konradt and Weder di Mauro (2023) do not find evidence for significant inflationary pressures caused by carbon taxes using data from European and Canadian carbon tax regimes.

I contribute to this literature by assessing the impact of EU ETS carbon price increases on emissions and the macroeconomy and using these results to estimate a New Keynesian macro-climate model with energy using Bayesian impulse response matching. Gagliardone and Gertler (2023) use a similar methodology to estimate a model to match the impulse responses to an oil shock. Their findings suggest that strong complementarity of oil in production and consumption are key to account for the macreconomic dynamics following an oil price increase. Sahuc et al. (2025) estimate a simple New Keynesian climate model without an explicit energy sector to analyze long-term transition scenarios under different climate policy regimes.

The second related strand of literature focuses on developing New Keynesian models with energy to assess the impact of carbon price increases on inflation and the conduct of monetary policy. Coenen et al. (2024) extend the ECB's New Area-Wide Model with a disaggregated energy sector to assess the impact of different carbon transition paths on the euro area economy. Their results suggest an increase in headline inflation and a fall in aggregate demand during the transition due to the increase in energy prices. Similarly, Olovsson and Vestin (2023) find that it is optimal for euro area monetary policy to see through increasing energy prices and focus on stabilizing core inflation, which leads to an increase in headline inflation. However, their results suggest that this increase is modest as long as the carbon tax path is pre-announced. Del Negro et al. (2023) develop a two-sector model to study how the green transition affects the central bank's trade-off between keeping prices stable and closing the output gap. Nakov and Thomas

(2023) study Ramsey optimal monetary policy in a model with climate externalities and how it is affected by different environmental policy regimes. I estimate a model with energy that is able to account for the gradual response in emissions, inflationary pressures and the significant fall in economic activity following a carbon price shock to assess the implications of climate change mitigation for the macroeconomy and monetary policy.

Structure. The remainder of the paper is structured as follows: Section 2 presents empirical evidence on the macroeconomic effects of a carbon price shock in the euro area. Section 3 introduces the New Keynesian macro-climate model with energy. Section 4 outlines the estimation methodology, presents the results and discusses key parameter specifications. Section 5 evaluates the impact of alternative monetary policy rules on the macroeconomic implications of carbon price shocks. Section 6 concludes.

2 Empirical Analysis

In this section, I assess the macroeconomic implications of an increase in the EU ETS carbon price in the euro area. The EU ETS operates as a carbon market where a fixed number of emission allowances are issued, granting firms the right to emit greenhouse gases (GHGs) into the atmosphere. Firms can buy, sell, and trade these allowances, creating a market-driven price for carbon emissions. To identify changes in the ETS price, I rely on the carbon price shock series developed by Känzig (2023), which captures unexpected variations in emission allowance futures prices using high-frequency surprise changes. It is a monthly shock series that spans from 1999 to 2019. I aggregate the monthly carbon price shock series up to a quarterly frequency to match the frequency of the data. I estimate the effects using simple local projections:

$$y_{i,t+h} = \beta^i_{h,0} + \gamma^i_h \, CPShock_t + \sum_{\ell=1}^{p} \beta^i_{h,\ell} \, y_{i,t-\ell} + \delta^i_h \, t + \epsilon_{i,t,h}, \tag{1}$$

where $CPShock_t$ denotes the ETS carbon price shock series. The coefficient γ^i_h measures the response of variable i at horizon h to a carbon price shock. I include three lags of the dependent variable as controls ($p = 3$). The term $\delta^i_h t$ accounts for linear trends over the sample. The estimation is based on quarterly euro area data from 1999Q1 to 2019Q4, focusing on the impact of carbon price increases on prices, greenhouse gas emissions, and real activity.

The variables included in the local projections are HICP energy inflation, headline HICP inflation, HICP inflation excluding energy, the real fossil energy price, greenhouse gas (GHG) emissions, industrial energy production, the short-term policy rate, real GDP, real private consumption, real investment, real wages, and capacity utilization. The real fossil energy price is constructed as a weighted index of the Brent crude oil price and

the HICP gas component, deflated by headline HICP. For the short-term policy rate, I splice the ECB policy rate with the shadow rate from Wu and Xia (2020) to account for the period when the policy rate was constrained by the zero lower bound. Since GHG emissions are only available annually, I construct a quarterly series using the Chow–Lin temporal disaggregation method with indicators, applying the code from Quilis (2024). Following Känzig (2023), I use the HICP energy component and industrial production as quarterly indicators. Inflation and the interest rate are expressed in annualized rates, while all other variables are measured in log-levels, except for capacity utilization.

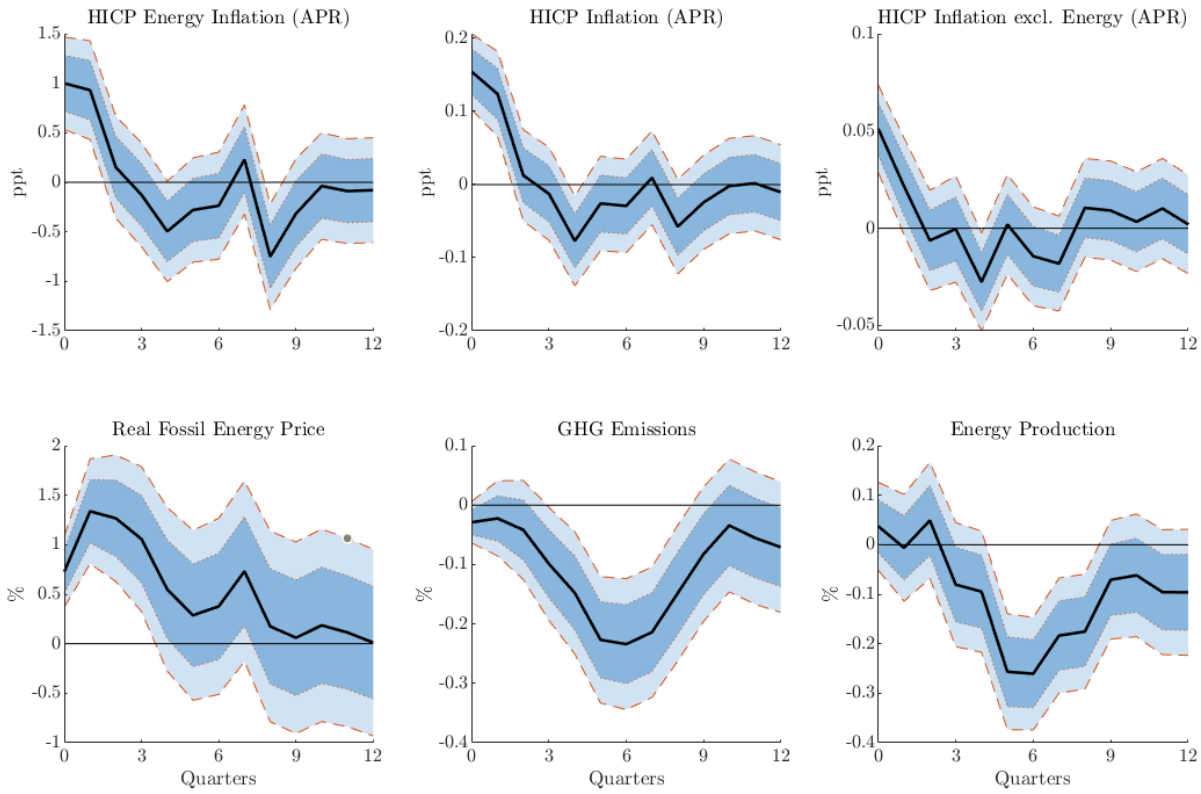

Figure 1: Impulse responses of prices, emissions and energy

The solid line is the point estimate, the dark and light shaded areas are 68 and 90 % confidence bands. The shock is normalized to increase annual energy inflation by 1 ppt.

Figure 1 shows the impulse responses to a carbon price shock for prices, GHG emissions, and industrial energy production. The shock is normalized to raise annualized energy inflation by one percentage point on impact, and confidence bands are computed using the lag-augmentation method of Montiel Olea and Plagborg-Møller (2021). The shock triggers an immediate rise in fossil energy prices and, consequently, aggregate energy prices. The pass-through of energy prices to consumer prices appears to be strong, as headline inflation increases by about 0.15 percentage points on impact. Inflation excluding energy also rises slightly, reflecting higher production costs being passed on to consumers. The carbon price increase proves effective in curbing emissions, with GHG emissions falling significantly by up to 0.25 percent. Interestingly, this adjustment does

not occur immediately but unfolds gradually, with the peak reduction materializing only a year after the shock. A very similar pattern is observed for industrial energy production, which contracts in response to the shock along almost the same trajectory. This co-movement is intuitive, as a large share of emissions originates from the combustion of fossil fuels in energy production. When higher carbon prices make fossil-based generation more costly, industrial energy output declines, and emissions fall in tandem. The delayed adjustment suggests that the reduction in fossil energy use unfolds gradually, leading both series to peak only with a lag. In terms of both direction and magnitude, these results are consistent with Känzig (2023) as well as previous evidence on different energy price shocks, such as oil shocks (Känzig (2021), Baumeister and Hamilton (2019)).

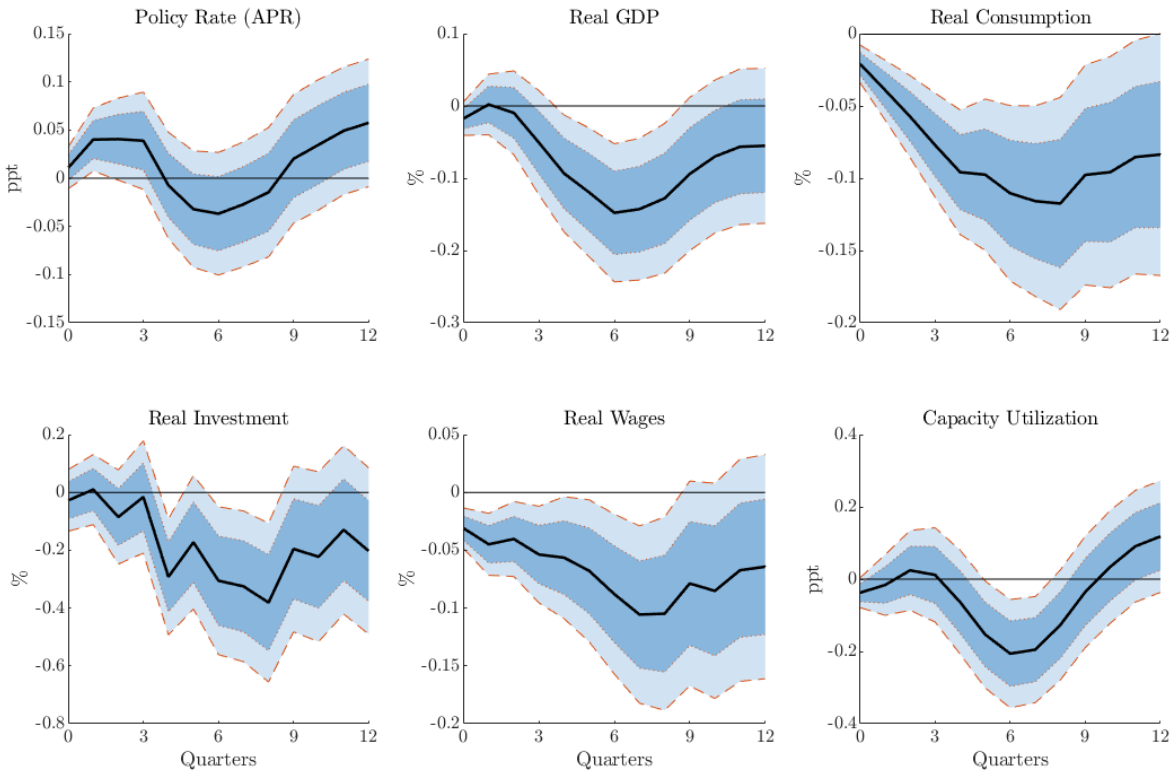

Figure 2: Impulse responses of macroeconomic aggregates

The solid line is the point estimate, the dark and light shaded areas are 68 and 90 % confidence bands. The shock is normalized to increase annual energy inflation by 1 ppt.

The results indicate a strong pass-through from fossil energy to consumer prices. Figure 2 presents the responses of several macroeconomic aggregates to the same carbon price shock. Real GDP declines significantly, with a peak reduction of about 0.15 percent, driven by contractions in both consumption and investment. Real wages and capacity utilization in production also fall. Higher energy prices directly reduce the disposable income of households and firms, lowering consumption and investment expenditure. This weakens output, which in turn creates incentives for firms to reduce labor costs. The delayed but significant decline in wages shown in Figure 2 illustrates this adjustment, and the resulting reduction in labor income further dampens aggregate demand. According

to Känzig (2023), such indirect general equilibrium effects account for more than two-thirds of the aggregate decline in consumption, helping explain the strong response of the real economy to the carbon price shock. Contractionary monetary policy in reaction to inflationary pressures from higher energy prices represents another potential channel, although the estimated policy rate response is small and largely insignificant. The decline in capacity utilization suggests that firms scale back production in response to higher energy costs.

The main results are robust to alternative specifications. Figure 10 presents estimates using four rather than three lags as controls ($p = 4$), which yield results very close to the baseline. Figure 11 in the Appendix reports impulse responses based on log-differences rather than log-levels to address potential concerns about non-stationarity. The local projections are estimated in log-differences and then aggregated to make the responses comparable to the baseline specification. The results in Figure 11 show that the point estimates are nearly identical to those in the baseline, while the confidence intervals are somewhat narrower for most variables.

3 The Model

The macro-climate model is a two-agent New Keynesian (TANK) framework extended by an energy sector. The economy is populated by ricardian and hand-to-mouth households, final good producers, intermediate good producers as well as producers of green and fossil energy. The production of fossil energy generates carbon emissions, while green energy production is carbon-neutral. Environmental damage from carbon emissions negatively affects total factor productivity. A bundle of green and fossil energy is used for both intermediate goods production and final consumption of households. Carbon policy is modeled as a surcharge on the price of fossil energy.

3.1 Households

The model features two types of households: Ricardian agents, denoted by subscript R, and hand-to-mouth agents, denoted by subscript H. R agents perform intertemporal optimization, have access to financial markets and supply capital and labor. Their preferences are specified as:

$$\mathbb{E}_0 \sum_{t=0}^{\infty} \beta^t \left\{ \log(c_{t,R} - b c_{R,t-1}) - \frac{h_{t,R}^{1+\varphi}}{1+\varphi} \right\}, \tag{2}$$

where $c_{t,R}$ represents final consumption, $h_{t,R}$ represents hours worked, $\beta \in (0,1)$ is the discount factor, b controls the degree of habit formation and φ is the inverse Frisch elasticity.

The R household's budget constraint is defined as follows in nominal terms:

$$\sum_j P_{t,R}c_{t,R} + P_t^I i_t^j + B_{t+1} = W_t h_{t,R} + (R_t^{k,j}u_t^j - a(u_t^j)P_t^I)k_{t-1}^j + R_{t-1}B_t + T_{t,R} + \Pi_t. \tag{3}$$

Here, $P_{t,R}$ is the price of final consumption goods and P_t^I is the price of investment goods $i_t^j, j \in (Y, G, B)$. Investment is allocated across three different sectors: capital goods for intermediate goods production k_t^Y, green energy production k_t^G and fossil energy production k_t^B. R_t^k is the nominal rental rate of capital and $u_t^j K_t^j$ denotes the household's supply of capital services in the given period, where u_t^j is the capacity utilization rate. $a(u_t^j)$ denotes cost of capacity utilization in units of investment goods. R households can invest in one-period risk-free bonds B_{t+1}, where $R_{t-1}B_t$ denotes the revenue from holding bonds. $W_t h_{t,R}$ is household R' labor income, $T_{t,R}$ are lump-sum transfers directed towards R agents and Π_t are firm profits.

Following Christiano et al. (2005), R households face quadratic adjustment costs in investment, so that investment is smoothed over time. This results in the following capital law of motion for each sector:

$$k_t^j = (1-\delta)k_{t-1}^j + \left[1 - \frac{\kappa_I}{2}\left(\frac{i_t^j}{i_{t-1}^j} - 1\right)^2\right] i_t^j, \quad j \in (Y, G, B) \tag{4}$$

where κ_I denotes the investment adjustment cost parameter.

Labor supplied by individual households is differentiated, which yields the following expression for aggregate labor supply:

$$h_{t,R} = \left(\int_0^1 h_{t,R}(i)^{\frac{\varepsilon_W - 1}{\varepsilon_W}} di\right)^{\frac{\varepsilon_W}{\varepsilon_W - 1}}, \tag{5}$$

where ε_W is the elasticity of substitution between individual varieties.

Ricardian households are assumed to set wages in a Calvo-style staggered fashion. Each period household i is able to reoptimize its nominal wage rate with probability $1 - \theta_W$. The remaining fraction of households cannot reoptimize, such that $W_t(i) = W_{t-1}(i)$ with probability θ_W.

The second type of households are hand-to-mouth, meaning they do not perform intertemporal optimization and have no access to financial markets, but instead consume all their disposable income in a given period. Their budget constraint reads as follows:

$$P_{t,H}c_{t,H} = W_t h_{t,H} + T_{t,H},$$

where $T_{t,H}$ are transfer payments directed towards H households. For simplicity, I assume that H agents have no bargaining power and do not optimize their hours worked, but instead work the same hours as R agents, $h_{t,H} = h_{t,R}$ to earn economy-wide wage W_t following Erceg et al. (2024). Including hand-to-mouth agents is crucial to account for potentially large demand-side effects of energy price shocks (see Auclert et al. (2023), Chan et al. (2024), Känzig (2023)).

To capture the energy consumption of households, final consumption $c_{t,j}$ is modeled as a CES bundle of energy ($c^E_{t,j}$) and the manufactured good from final good production ($c^X_{t,j}$), such that

$$c_{t,j} = \left(\gamma_{c,j}^{\frac{1}{\varrho_c}} (c^E_{t,j})^{\frac{\varrho_c - 1}{\varrho_c}} + (1 - \gamma_{c,j})^{\frac{1}{\varrho_c}} (c^X_{t,j})^{\frac{\varrho_c - 1}{\varrho_c}} \right)^{\frac{\varrho_c}{\varrho_c - 1}}, \; j \in \{H, R\}. \tag{6}$$

Here, $\gamma_{c,j}$ determines the share of energy in final consumption, which is heterogeneous across household types, and ϱ_c is the elasticity of substitution between energy and the manufactured good. The resulting demand equations for energy and the manufactured consumption good are:

$$c^E_{t,j} = \gamma_{c,j} \left(\frac{P^E_t}{P_{t,j}} \right)^{-\varrho_c} c_{t,j}, \tag{7}$$

$$c^X_{t,j} = (1 - \gamma_{c,j}) \left(\frac{P^X_t}{P_{t,j}} \right)^{-\varrho_c} c_{t,j}, \tag{8}$$

where P^E_t and P^X_t are their respective prices. The CPI can therefore be defined such that it captures both goods and energy prices:

$$P_{t,j} = \left(\gamma_{c,j} (P^E_t)^{1-\varrho_{c,j}} + (1 - \gamma_c)(P^X_t)^{1-\varrho_c} \right)^{\frac{1}{1-\varrho_c}}. \tag{9}$$

Based on this specification, headline inflation π_t is given by:

$$\pi_t = \frac{p_t}{p_{t-1}} \pi^X_t, \tag{10}$$

where p_t denotes the headline CPI in terms of core CPI. π^X_t defines core inflation, which excludes fluctuations in energy prices.
Similarly, energy inflation is defined as follows:

$$\pi^E_t = \frac{p^E_t}{p^E_{t-1}} \pi^X_t. \tag{11}$$

3.2 Final good firms

The representative final-good firm uses the following CES bundle to produce the final good y_t:

$$y_t = \left(\int_0^1 y_t(i)^{\frac{\varepsilon-1}{\varepsilon}} di \right)^{\frac{\varepsilon}{\varepsilon-1}}, \tag{12}$$

where $y_t(i)$ is an intermediate good produced by intermediate good firm i and ε is the elasticity of substitution between intermediate goods. The profit maximization problem of the final good firm reads as follows:

$$\max_{y_t, \{y_t(i)\}_{i\in[0,1]}} P_t^X y_t - \int_0^1 P_t^X(i) y_t(i) di \tag{13}$$

$$\text{s.t.} \quad y_t = \left(\int_0^1 y_t(i)^{\frac{\varepsilon-1}{\varepsilon}} di \right)^{\frac{\varepsilon}{\varepsilon-1}}. \tag{14}$$

Here, $P_{H,t}(i)$ is the price of the intermediate good produced by firm i in the home country. The problem yields the following intermediate input demand:

$$y_t(i) = \left(\frac{P_t^X(i)}{P_t^X} \right)^{-\varepsilon} y_t. \tag{15}$$

3.3 Intermediate good firms

A continuum of intermediate goods $y_t(i)$ is produced by price setting firms that are optimizing under monopolistic competition. The production function of these firms is a CES aggregator in energy and value added from a Cobb-Douglas bundle of capital and labor, following Hassler et al. (2021):

$$y_t(i) = A_t^Y \left[(1-\gamma_Y)^{\frac{1}{\varrho_Y}} \left((u_t^Y k_{t-1}^Y(i))^{\alpha} (h_t^Y(i))^{1-\alpha} \right)^{\frac{\varrho_Y-1}{\varrho_Y}} + (\gamma_Y)^{\frac{1}{\varrho_Y}} \left(e_t^Y(i) \right)^{\frac{\varrho_Y-1}{\varrho_Y}} \right]^{\frac{\varrho_Y}{\varrho_Y-1}}, \tag{16}$$

where $e_t^Y(i)$, $u_t^Y k_{t-1}^Y(i)$ and $h_t^Y(i)$ respectively is the energy, effective capital and labor demanded by firm i, α is the capital share in the value added from capital and labor, γ_Y is the energy share in intermediate goods production and ϱ_Y is the elasticity of substitution between energy and the capital-labor bundle.

Firms set their price P_t^X and choose input factors capital, labor and energy to maximize profits subject to their production technology (16) and the demand of the final good firm (15).The firms set prices in Calvo-style staggered contracts, such that each firm faces a constant probability $1-\theta_P$ of being able to adjust its price. The remaining firms that are not able to reoptimize set their price according to $P_t^X(i) = P_{t-1}^X(i)$.

3.4 Energy sector

A representative energy firm combines two different energy sources, green energy e_t^G and fossil energy e_t^F, to provide energy services to households and for intermediate goods production. The energy inputs are bundled using the following CES aggregator:

$$e_t = \left((1-\zeta)^{\frac{1}{\xi}}(e_t^G)^{\frac{\xi-1}{\xi}} + \zeta^{\frac{1}{\xi}}(e_t^F\ (1-\Gamma_t))^{\frac{\xi-1}{\xi}}\right)^{\frac{\xi}{\xi-1}}, \tag{17}$$

where ξ is the elasticity of substitution between green and fossil energy and ζ determines the share of fossil energy in energy production. The energy firm faces quadratic adjustment costs Γ_t in fossil energy:

$$\Gamma_t = \frac{\kappa_E}{2}\left(\frac{e_t^F}{e_{t-1}^F} - 1\right)^2. \tag{18}$$

These costs are crucial to account for the slow adjustment of fossil energy use following a carbon price increase, for instance due to long-term contracts with fossil fuel providers or the lack of appropriate infrastructure to switch to renewable energy sources.

The respective demand equations for fossil and green energy are:

$$e_t^F = \zeta\left(\frac{(1+\tau_t)p_t^F}{(1-\Gamma_t-\Gamma_t' e_t^F)p_t^E}\right)^{-\xi}\frac{e_t}{1-\Gamma_t}, \tag{19}$$

$$e_t^G = (1-\zeta)\left(\frac{p_t^G}{p_t^E}\right)^{-\xi} e_t, \tag{20}$$

where the carbon policy rate τ_t is modeled as a surcharge on the price of fossil energy. This implies a trade-off for energy firms. Higher carbon prices create an incentive for energy firms to reduce fossil fuel use to lower production costs. However, the firms face adjustment costs, preventing large and abrupt cuts in fossil energy use. I model carbon policy as a carbon tax for simplicity, because both carbon taxes and cap-and-trade systems like the EU ETS increase the price of fossil fuel use to reduce emissions. The carbon tax rate follows an AR(1) process:

$$\log(\tau_t) = (1-\rho_\tau)\log(\overline{\tau}) + \rho_\tau \log(\tau_{t-1}) + \epsilon_t^\tau, \tag{21}$$

where ϵ_t^τ is an exogenous carbon price shock and $\overline{\tau}$ is the steady state carbon tax rate.

Both energy inputs are produced using a Cobb-Douglas bundle of sector-specific capital and labor services k_t^j and h_t^j, $j \in \{F, G\}$:

$$e_t^j = A_t^j (u_t^j k_{t-1}^j)^\alpha (h_t^j)^{1-\alpha}, \quad j \in \{F, G\}, \tag{22}$$

where u_t^j is the sector-specific rate of capacity utilization.

Fossil energy production generates carbon emissions m_t, such that:

$$m_t = \vartheta e_t^F, \tag{23}$$

where ϑ determines the carbon content of fossil energy production.

3.5 Monetary and fiscal policy

The fiscal authority levies the carbon tax on energy firms and rebates the revenues to Ricardian households through lump-sum transfers. This provides a neutral benchmark for revenue use, consistent with the EU ETS, where revenues are intended either to finance environmental projects or to be returned to households, with allocation left to the discretion of member states. I abstract from the existence of public debt and assume the fiscal authorities run a balanced budget at all times. The government budget constraint takes the following form:

$$\tau_t p_t^B e_t^B = T_t + g, \tag{24}$$

where government spending g is assumed to be constant.

The central bank follows a Taylor rule to set the nominal interest rate r_t:

$$\frac{r_t}{r} = \left(\frac{r_{t-1}}{r}\right)^{\rho_r} \left[\left(\frac{\pi_t}{\pi}\right)^{\phi_\pi} \left(\frac{gdp_t}{gdp}\right)^{\phi_y}\right]^{(1-\rho_r)}, \tag{25}$$

In the baseline analysis, the central bank is assumed to respond to deviations in headline HICP inflation and output.

3.6 Climate change

I introduce a climate change externality as in Golosov et al. (2014) into my model to capture negative effects of increasing atmospheric carbon on the economy. The externality creates a two-way interaction between the economy and climate change. In the benchmark model, fossil energy production generates carbon emissions, which feed into the stock of atmospheric carbon. The stock of atmospheric carbon evolves according to the following process:

$$S_t = (1 - \delta_S) S_{t-1} + (m_t + m^{row}), \tag{26}$$

where $\delta_{S,0}$ is the depreciation rate of carbon dioxide from the atmosphere and $\delta_{S,1}$ is the percentage of carbon emissions that enter the atmosphere. The global stock of atmospheric carbon is fueled by domestic euro area emissions m_t and emissions from the rest

of the world m^{row}, which is constant over time, because I assume no climate policy action in the rest of the world.

The extended model now introduces a feedback effect, such that the environmental damage from higher atmospheric carbon reduces total factor productivity.[1]. Following Golosov et al. (2014), total factor productivity in each production sector is then modeled as follows:

$$A_t^i = a_t^i e^{-\psi_D S_t}, \qquad i \in \{Y, G, B\}, \tag{27}$$

where ψ_D is the damage parameter that determines the size of the externality and $a_t^i, i \in \{Y, G, B\}$ is the total factor productivity that would prevail in each sector without the environmental externality.[2]

3.7 Market clearing and functional forms

The labor and energy market clear such that:

$$h_t = h_t^Y + h_t^B + h_t^G, \tag{28}$$

$$e_t = \lambda c_{t,H}^E + (1-\lambda) c_{t,R}^E + e_t^Y, \tag{29}$$

where λ denotes the share of hand-to-mouth agents.
Aggregate investment is defined as follows:

$$i_t = i_t^Y + i_t^B + i_t^G. \tag{30}$$

Aggregating firm profits implies:

$$\Pi_t = \Pi_t^Y + \Pi_t^F + \Pi_t^G. \tag{31}$$

The resource constraint of the economy is then obtained by plugging the government budget constraint and the profit functions of intermediate goods firms and energy producers into the weighted sum of household budget constraints:

$$y_t = c_t^X + i_t + g + \sum_j a(u_t^j) k_{t-1}^j, \quad j \in \{Y, B, G\}. \tag{32}$$

[1] Antoher approach of some environmental DSGE models is to include the pollution externality directly into the utility function of households (see Acemoglu et al. (2012), Benmir et al. (2020), Barrage (2020)). However, Nordhaus (2008) and Heutel (2012) argue that such a modeling choice would be more appropriate for conventional pollutants that directly affect health rather than greenhouse gases.

[2] For simplicity, this is set to $a_t^i = 1$ in each sector.

Real GDP is measured as follows:

$$gdp_t = p_t c_t + i_t + g, \tag{33}$$

where aggregate consumption expenditure is defined as:

$$p_t c_t = \lambda p_{t,H} c_{t,H} + (1-\lambda) p_{t,R} c_{t,R}. \tag{34}$$

The capacity utilization adjustment cost function is defined as:

$$a(u) = \frac{1}{2}\sigma_0 \sigma_a u^2 + \sigma_0(1-\sigma_a)u + \sigma_0\left(\frac{1}{2}\sigma_a - 1\right), \tag{35}$$

where σ_0 is set such that $a(1) = a'(1) = 0$ in steady state. The parameter σ_a controls the curvature of the adjustment cost function, such that a higher σ_a indicated larger costs for changing capacity utilization.

A full set of equilibrium equations as well as the steady state of the model is listed in appendix A.

4 Estimation Results

I estimate the key parameters of the model by matching the dynamic responses to a carbon price shock in the model with the estimated impulse responses from the data presented in section 2 using Bayesian impulse response matching. First, I calibrate a set of parameters and then estimate the remaining parameters conditional on the set of calibrated parameters.

4.1 Estimation methodology

For the estimation I follow the limited information Bayesian methodology developed in Christiano et al. (2010) that minimizes the distance between the dynamic impulse responses to the carbon price shock ϵ_τ in the model and the analog responses in the data. The impulse responses from the data are estimated using local projections in section 2. I use ten of the variables considered in the local projections for the estimation procedure: real fossil energy prices, energy inflation, headline inflation, nominal interest rate, emissions, real GDP, real consumption, real investment, real wages and capacity utilization.

The estimation procedure relies on the assumption that the structural model correctly describes the data-generating process. Let θ_0 denote the true values of the model parameters, and let $\psi(\theta)$ represent the mapping from the parameter space to the model-implied impulse responses. Then, $\psi(\theta_0)$ corresponds to the true impulse responses, which are

estimated from the data as $\hat{\psi}$. Under standard asymptotic sampling theory, when the number of observations T is large, the empirical impulse responses satisfy:

$$\sqrt{T}\left(\hat{\psi} - \psi(\theta_0)\right) \overset{d}{\sim} N(0, W(\theta_0, \zeta_0)). \tag{36}$$

Here, θ_0 represents the true values of the model parameters, while ζ_0 denotes the true values of shocks that are not explicitly estimated. The vector $\hat{\psi}$ includes the contemporaneous and 11 lagged responses of the 10 variables used for the estimation. The asymptotic distribution of $\hat{\psi}$ can be rewritten as:

$$\hat{\psi} \overset{d}{\sim} N(\psi(\theta_0), V), \tag{37}$$

where $V = W(\theta_0, \zeta_0)/T$. In practice, I use a consistent estimator for V, considering only diagonal elements, as suggested by Christiano et al. (2010).

To estimate the model parameters, I treat $\hat{\psi}$ as observed data and specify prior distributions for θ. Using Bayes' theorem, I compute the posterior distribution of θ given $\hat{\psi}$ and V. The likelihood function for $\hat{\psi}$ given θ is approximated by:

$$f(\hat{\psi}|\theta, V) = (2\pi)^{-N/2}|V|^{-1/2} \exp\left[-0.5(\hat{\psi} - \psi(\theta))'V^{-1}(\hat{\psi} - \psi(\theta))\right]. \tag{38}$$

Maximizing this function provides an approximate maximum likelihood estimator for θ. The likelihood function is derived from the asymptotic distribution of the impulse responses and accounts for estimation uncertainty. I obtain parameter estimates by maximizing the posterior density and use a Markov Chain Monte Carlo (MCMC) algorithm to sample from the posterior distribution.

4.2 Calibrated parameters

The model is calibrated to the euro area at a quarterly frequency. All calibrated parameter values are shown in Table 1.

The quarterly discount factor is set to $\beta = 0.995$, which implies an annual steady-state real interest rate of 2%. The steady-state inflation rate is calibrated to match an annual inflation of 2% for both core and headline inflation. The substitution elasticity between intermediate goods is set to $\varepsilon = 6$, which is a standard value in New Keynesian models, implying a gross steady-state price mark-up of $\mu_P = \frac{\varepsilon}{\varepsilon - 1} = 1.2$. The gross steady-state wage mark-up is also set to $\mu_W = 1.2$. The capital share in production is set to $\alpha = 0.3$ and capital depreciates at a rate of $\delta = 2.5\%$ each quarter. The inverse Frisch elasticity is set to $\varphi = 1$.

The energy-related parameters are calibrated to match euro area data in steady state. The share of energy in the consumption bundle, $\omega^j_{e,c}$ for $j \in R, H$, is set to replicate households' energy expenditure shares in the euro area. According to Eurostat, these

Table 1: Calibrated parameters

Parameter	Description	Value	Source
$(p^E c_{e,R})/(p_R c_R)$	Energy share in consumption R	0.07	Eurostat, HFCS (2015)
$(p^E c_{e,H})/(p_H c_H)$	Energy share in consumption H	0.16	Eurostat, HFCS (2015)
$(p^E e^Y)/(p^C y)$	Energy share in production	0.07	Coenen et al. (2024)
e^G/e	Green energy share	0.15	Eurostat
β	Discount factor	0.995	Annual real rate 2%
φ	Inverse Frisch elasticity	1	Standard value
α	Capital share in production	0.3	Standard value
δ	Depreciation rate	0.025	Standard value
μ_P	Gross st.-st. price mark-up	1.2	Standard value
μ_W	Gross st.-st. wage mark-up	1.2	Standard value
δ_S	Decay atmospheric carbon	0.9983	Hassler et al. (2020)
$100 \cdot \psi_D$	Damage coefficient	0.002698	Hassler et al. (2020)

shares are about 16 percent for households in the bottom income quartile and 7 percent for the remaining households. This calibration implies an economy-wide average energy expenditure share of roughly 9 percent, which is consistent with the HICP weight for energy. The distribution parameter $\gamma_{c,j}$ is then calibrated to ensure this expenditure share of every value of p^E and ϱ_c in steady state:

$$\gamma_{c.j} = \omega_{e,c}^{j} (p^E)^{\varrho_c - 1}. \tag{39}$$

Similarly, $\omega_{e,y}$ matches the share of energy in production of about 7% in the euro area following Coenen et al. (2024). such that:

$$\gamma_c = \omega_{e,y} \left(\frac{p^E}{p^X} \right)^{\varrho_y - 1}. \tag{40}$$

The steady-state share of green energy in aggregate energy production is set to $\zeta = 15\%$, reflecting the average value for the euro area for the sample period of 1999 to 2019.

Finally, for the calibration of the climate module, I follow the estimates from Hassler et al. (2020). The damage function coefficient ψ_D is estimated to specifically capture damages from carbon-induced temperature increases in Europe.

4.3 Estimated parameters and results

Conditional on the calibrated parameters, I then estimate the remaining fifteen model parameters. Table 2 reports the prior and posterior distributions of the estimated parameters. This section discusses the estimated parameter values and their implications, with a particular focus on the energy-related parameters.

First, the results imply strong complementarity between energy and other inputs in

Table 2: Priors and Posteriors of Parameters

Parameter	Prior	Posterior	
	$\mathcal{D}$, Mode [5-95%]	Mode	[5-95%]
Energy complementarity firms, ϱ_y	$\mathcal{G}$, 0.32 [0.13 1.07]	**0.07**	[0.02 0.20]
Energy complementarity households, ϱ_c	$\mathcal{G}$, 0.32 [0.13 1.07]	**0.12**	[0.04 0.29]
Substitution green and fossil energy, ξ	$\mathcal{U}$, – [0.2 3.8]	**0.38**	[0.23 0.72]
Fossil energy adjustment cost, κ_E	$\mathcal{U}$, – [1.5 28.5]	**10.1**	[6.4 16.3]
Share of hand-to-mouth agents, λ	$\mathcal{B}$, 0.28 [0.15 0.48]	**0.25**	[0.16 0.39]
Habit persistence, b	$\mathcal{B}$, 0.63 [0.34 0.83]	**0.73**	[0.43 0.88]
Calvo wage stickiness, θ_w	$\mathcal{B}$, 0.76 [0.43 0.92]	**0.84**	[0.60 0.96]
Investment adjustment costs, κ_I	$\mathcal{G}$, 3.20 [1.27 10.73]	**3.65**	[0.28 8.50]
Capacity utilization adj. costs, κ_U	$\mathcal{G}$, 0.44 [0.15 2.46]	**0.22**	[0.03 1.02]
Calvo price stickiness, θ_p	$\mathcal{B}$, 0.76 [0.43 0.92]	**0.61**	[0.35 0.81]
Taylor rule inflation coeff., ϕ_π	$\mathcal{G}$, 1.58 [1.36 1.84]	**1.53**	[1.25 1.88]
Taylor rule output coeff., ϕ_y	$\mathcal{G}$, 0.04 [0.01 0.26]	**0.04**	[0.00 0.15]
Interest rate smoothing, ρ_r	$\mathcal{B}$, 0.85 [0.61 0.94]	**0.95**	[0.90 0.99]
Autocorr. carbon shock, ρ_τ	$\mathcal{B}$, 0.75 [0.44 0.95]	**0.90**	[0.85 0.95]
Std.Dev. carbon shock, σ_τ	$\mathcal{IG}$, 0.07 [0.04 0.56]	**0.26**	[0.21 0.35]

Notes: Posterior mode and intervals are based on a standard MCMC algorithm with 500,000 draws (5 chains, 50% burn-in, acceptance rate about 27%). $\mathcal{B}, \mathcal{G}, \mathcal{U}, \mathcal{IG}$ denote beta, gamma, uniform and inverse-gamma distributions, respectively.

production as well as energy and non-energy goods in consumption. This complementarity is a standard assumption in macro climate models with energy with values usually ranging between 0.2 and 0.5 (Hassler et al. (2021), Coenen et al. (2024), Diluiso et al. (2021)). My estimates are lie slightly below this range with $\varrho_c = 0.12$ and $\varrho_y = 0.07$. The 90% interval is also on the lower end of estimates in the literature. Such a high degree of complementarity makes households and firms very vulnerable to carbon price shocks, because the sharp increase in energy prices will increase their energy bills, leading to a significant drop in consumption and investment expenditure. These results are in line with Gagliardone and Gertler (2023) who estimate strong complementarities of oil in production and consumption using an oil price shock.

Second, the posterior mode of the substitution elasticity between green and fossil energy is estimated at $\xi = 0.38$. Since this value is well below unity, it implies that green and fossil energy behave as complements rather than substitutes in aggregate energy production. The 90% confidence interval places an upper bound at 0.72, reinforcing the conclusion that the two inputs are complements. Standard values in the literature typically range from 1.8 to 3, suggesting much higher substitutability (Papageorgiou et al. (2017), Coenen et al. (2024)). The relatively low estimate obtained here reflects that the identification strategy captures a short-term substitution elasticity following temporary carbon price shocks, rather than long-term adjustment dynamics in response to permanent carbon price increases. The substitution elasticity remains a key parameter

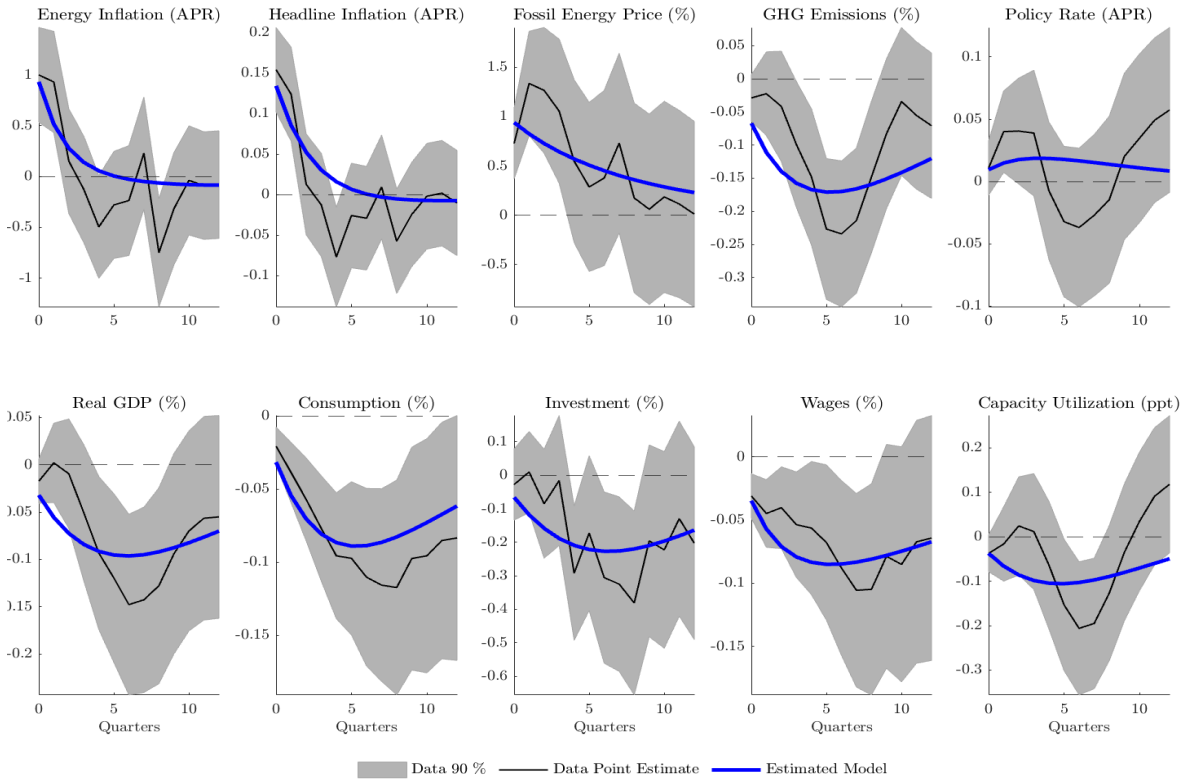

Figure 3: Impulse responses to carbon price shock: Model vs. Data

for assessing the effectiveness of carbon pricing policies.

Third, the posterior mode of the fossil energy adjustment cost parameter is significantly positive with $\kappa_E = 10.1$. These types of adjustment costs are non-standard in New Keynesian climate models, implying a value of $\kappa_E = 0$. My results suggest that including adjustment costs in the share of fossil energy is crucial to match the lagged response of emissions following an increase in the carbon price. Section 4.4 provides a detailed analysis of the implications of the parameter estimates for ξ and κ_E.

Finally, the estimated posterior mode of the population share of hand-to-mouth households is $\lambda = 0.25$. This indicates that accounting for hand-to-mouth households is important in order to match the observed response of the economy to the shock. The estimate is also consistent with previous findings for the euro area (Dossche et al. (2021)).

The remaining parameters, that are not directly related to the energy sector, fall within a reasonable range for standard macroeconomic models. The degree of price stickiness suggests that prices are adjusted every three quarters on average, while nominal wages remain unchanged for about eight quarters on average. Habit persistence $b = 0.73$ is slightly higher, but still close to the estimate of the New Area Wide Model (Coenen et al. (2018), henceforth NAWM II). Investment and capacity utilization adjustment costs are a little lower than suggested by the NAWM II. The estimated Taylor rule coefficients suggest a high degree of interest rate smoothing and a small coefficient on output growth, while the output gap coefficient is close to zero, which is also in line with the NAWM II.

The persistence of the carbon price shock is approximately $\rho_\tau = 0.9$.

Figure 3 compares the dynamic impulse responses from the model, depicted by the blue line, to the responses estimated from the data in section 2, depicted by the black line. The grey areas are the 90% confidence intervals from the local projections. The model adequately captures the dynamics observed in the data following a carbon price shock. As aggregate energy prices are a bundle of fossil and green energy prices, the carbon price increase leads to a surge in energy inflation. This leads to a rise in headline inflation, both due to a direct increase in households' energy expenditure and due to firms passing on higher production costs to consumers. Higher energy bills directly lead to lower consumption and investment expenditure. The increase in production costs of firms leads to a decline in wages and capacity utilization. Lower wages in turn further decrease aggregate demand. The negative effects on aggregate demand are amplified by the rise in real interest rates as monetary policy leans against inflationary pressures.

4.4 Counterfactual analysis

This section examines the role of three key parameters—the substitution elasticity between green and fossil energy (ξ), the fossil energy adjustment cost parameter (κ_E), and the share of hand-to-mouth agents (λ). The first two parameters determine how flexibly firms and households can adjust their energy use and how smoothly the economy transitions away from fossil fuels in response to policy changes, while λ governs the share of the population that is particularly vulnerable to energy price increases. To illustrate how these parameters shape model dynamics, I fix all estimated parameters at their posterior modes (as reported in Table 2) and simulate three counterfactual scenarios: (i) no fossil energy adjustment costs ($\kappa_E = 0$), (ii) higher substitutability between green and fossil energy ($\xi = 3$), and (iii) a representative-agent economy ($\lambda = 0$). I then re-estimate the model under each counterfactual and compare the resulting impulse responses to the baseline estimates shown in Figure 3.

Figure 4 illustrates Scenario (i), which sets the fossil energy adjustment cost parameter to zero. The strongest effect appears in aggregate energy prices: energy inflation spikes by more than 3 percentage points on impact, which is over three times the response observed in the data. This surge quickly feeds through to headline inflation, which rises by around 0.4 percentage points, amplifying short-run cost pressures across the economy. Because energy firms can immediately substitute away from fossil energy use in this scenario, emissions fall sharply on impact. As a result, the model fails to capture the gradual and persistent decline in emissions observed in the data. In reality, adjustment frictions such as infrastructure limitations, supply constraints, and technology adoption barriers slow the transition away from fossil fuels, dampening the short-run response.

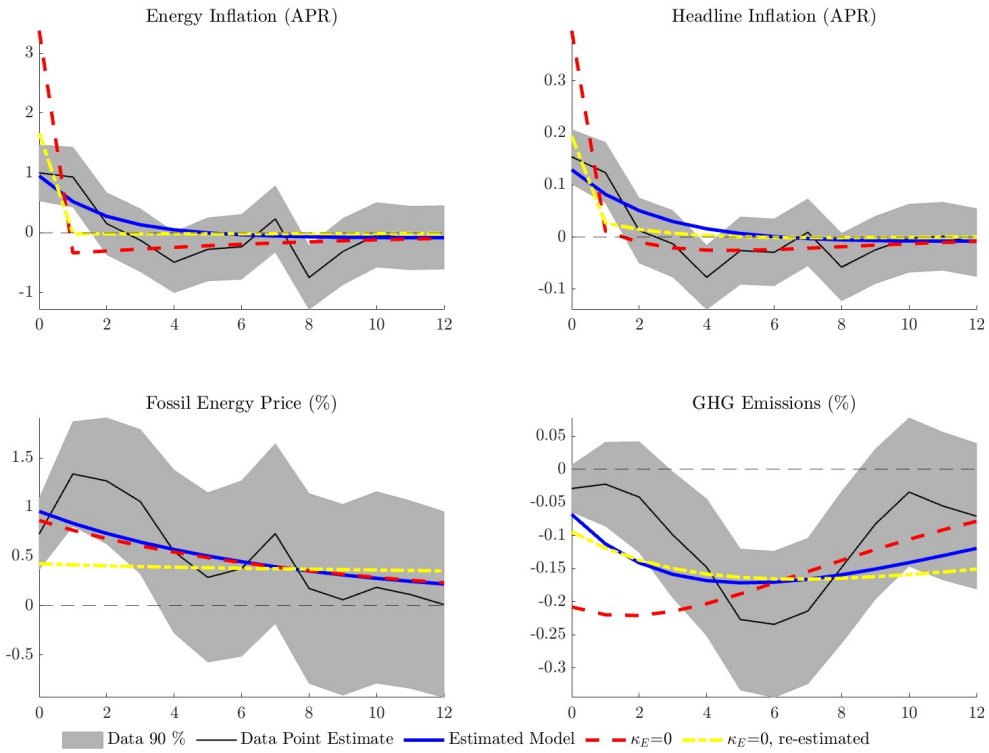

Figure 4: Impulse responses to carbon price shock: Baseline ($\kappa_E = 10.1$) vs. $\kappa_E = 0$

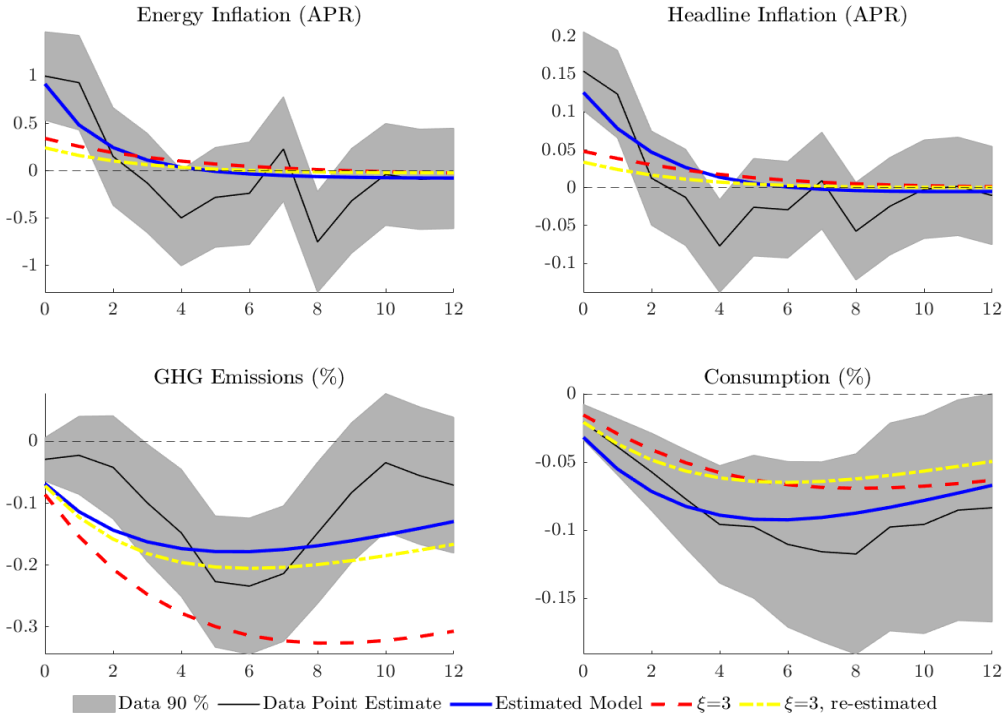

Figure 5: Impulse responses to carbon price shock: Baseline ($\xi = 0.38$) vs. $\xi = 3$

Re-estimating the model without fossil energy adjustment costs yields inflation responses closer to the data. However, matching the gradual decline in emissions requires

assuming a highly persistent shock, which is reflected in the response of fossil energy prices. The fossil energy price increases by roughly 0.5 percent on impact, which is below the empirical estimate, and remains unchanged for almost three years.

Figure 4 illustrates Scenario (ii), which sets the substitution elasticity between green and fossil energy to $\xi = 3$. A higher elasticity implies that energy producers can more easily substitute away from fossil energy, which dampens the sharp impact response of aggregate energy inflation. As a result, the rise in headline inflation is substantially muted, alleviating some of the short-run cost pressures on households. This, in turn, leads to a noticeably smaller contraction in consumption compared to the baseline estimated model. At the same time, greater substitutability accelerates the shift toward green energy, producing a stronger and more immediate reduction in emissions than observed in the data. While re-estimating the model under this higher substitutability can account for the smaller decline in emissions, it comes at the cost of generating an even weaker response of headline inflation.

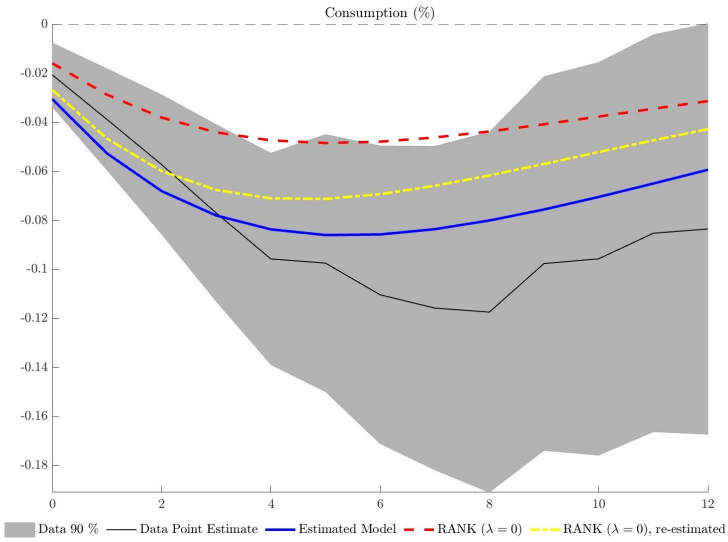

Figure 6: Impulse responses to carbon price shock: Baseline (TANK, $\lambda = 0.25$) vs. RANK, $\lambda = 0$

Figure 6 compares the impulse response of consumption in the baseline TANK model to a standard RANK model where all households are Ricardian. Hand-to-mouth households spend a relatively larger share of their income on energy than Ricardian agents. In addition, since they consume all disposable income in a period, they cannot self-insure against adverse shocks. A model that does not include these types of agents cannot reproduce the significant fall in private consumption observed in the data.

5 Monetary Policy

While central banks do not directly engage in climate change mitigation, they must respond to the macroeconomic consequences of carbon pricing. As shown above, a carbon price shock raises inflation while reducing output, creating a monetary policy trade-off.[3] This section examines the optimal monetary policy response to such a shock and compares how alternative policy rules shape the transmission of carbon pricing to the macroeconomy.

5.1 Optimal Monetary Policy

In the optimal policy regime, the central bank acts as a benevolent planner that chooses the optimal trajectory of the nominal interest rate $\{r_t\}$ to maximize social welfare from a timeless perspective:

$$\max \mathcal{W}_t = \mathbb{E}_0 \sum_{t=0}^{\infty} \beta^t \left[\lambda(\mathcal{U}_t^H) + (1-\lambda)(\mathcal{U}_t^R) \right], \tag{41}$$

subject to the private sector constraints from the firm's profit maximizing and household's utility maximizing behavior and the path of the carbon price. The central bank is assumed to commit to the contingent policy rule announced at time 0, which allows dynamic adjustment of the policy instrument to changing economic conditions. Note that I consider a second-best allocation as in Schmitt-Grohé and Uribe (2004) due to inefficiency in the initial steady state, arising from distortive monopolistic competition in intermediate-goods production and wage setting.

In addition, to assess the implications of an alternative interest rate rule, I analyze the implications of a policy rule that focusses on stabilizing core inflation π_t^X instead of headline inflation:

$$\frac{r_t}{r} = \left(\frac{r_{t-1}}{r}\right)^{\rho_r} \left[\left(\frac{\pi_t^X}{\pi}\right)^{\phi_\pi} \left(\frac{gdp_t}{gdp}\right)^{\phi_y} \right]^{(1-\rho_r)}. \tag{42}$$

The reaction coefficients in this specification are the same as in the baseline estimated model.

Figure 7 compares the impulse responses to a carbon price shock in the baseline estimated model to the two alternative monetary policy regimes. The optimal policy response to a carbon price shock differs markedly from the baseline Taylor rule that targets headline inflation. The Ramsey planner places substantial weight on stabilizing output

[3]This trade-off can also be observed empirically. Figure 12 in the Appendix shows no significant response of potential output to the shock, while the output gap and real GDP react in a very similar way in terms of direction and magnitude.

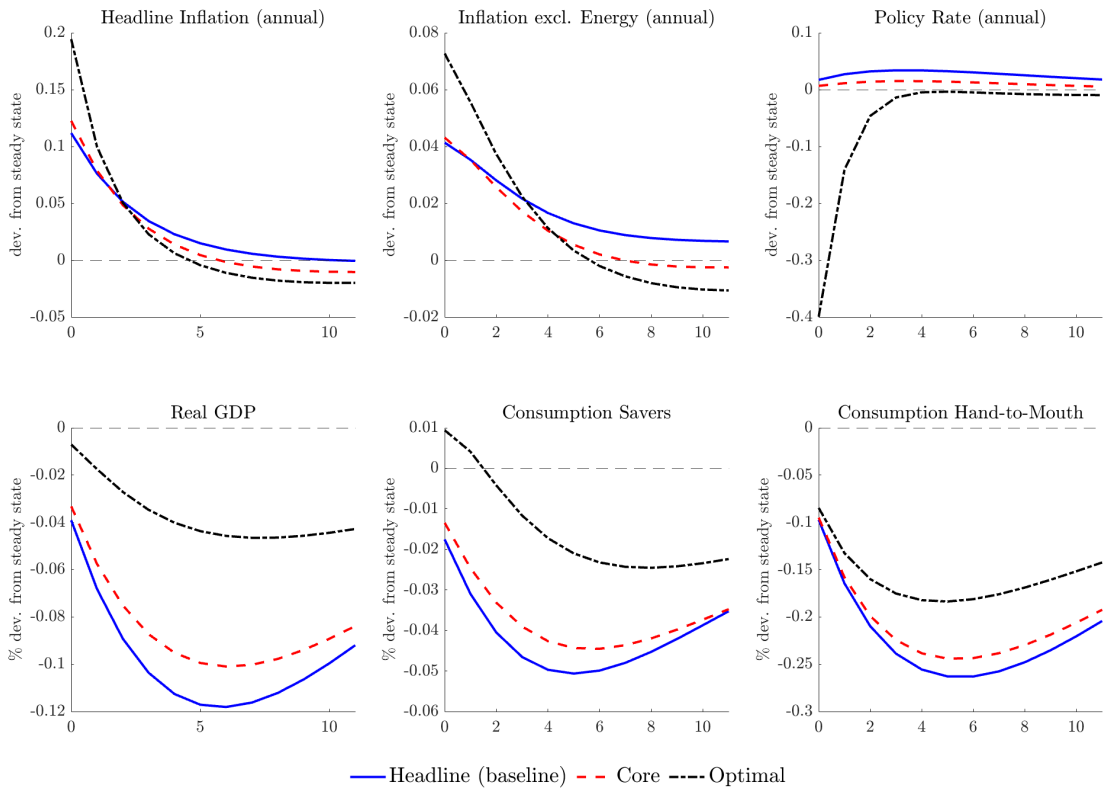

Figure 7: Impulse responses to a carbon price shock: Optimal monetary policy vs. headline inflation stabilization vs. core inflation stabilization

rather than fully offsetting the rise in prices. While the shock raises headline inflation, it also generates a sharp contraction in GDP and consumption. These output losses arise because energy is a critical input across the economy: fossil and green energy are not easily substitutable in energy production, energy itself enters production of intermediate goods in a complementary way, and households have limited scope to substitute energy use in consumption. As a result, higher fossil energy prices translate into higher costs for households and firms, which leads to lower labor demand, and suppressed wages, which in turn reduce disposable income. In this environment, an aggressive interest rate increase to contain inflation would amplify the fall in demand and lead to larger welfare losses.

Instead, the planner cuts the policy rate sharply, thereby strongly mitigating the fall in output and consumption. This comes at the cost of temporarily higher headline and core inflation. In other words, the planner accepts inflationary pressures, focusing instead on stabilizing aggregate demand. The sharp initial interest rate cut is strongly driven by the significant fall in hand-to-mouth consumption in response to the shock. As hand-to-mouth households spend a relatively larger fraction of their disposable income on energy and cannot self-insure against adverse shocks, they are hit substantially harder by the shock than Ricardian households. Figure 13 in the Appendix shows that if the planner only maximizes welfare based on Ricardian agents' utility, the interest rate trajectory is much smoother. However, the planner in this scenario still clearly favors output

stabilization over inflation stabilization.

When monetary policy follows a rule that targets core rather than headline inflation, the results come closer to the optimal response. Because core inflation excludes volatile energy prices, the central bank reacts less aggressively to the initial rise in headline inflation. This moderates the rise in real interest rates and thereby the contraction in output and consumption relative to the headline-based rule. While this comes at the cost of a slightly stronger initial increase in headline inflation, this effect is very small. In this sense, a core inflation rule approximates the Ramsey allocation more closely, as it implicitly places less weight on energy-driven price movements and thereby more on stabilizing the real economy, while not strongly increasing inflation volatility.

Overall, these results highlight that monetary policy faces a clear trade-off in responding to carbon price shocks. Policies that mechanically target headline inflation risk exacerbating inefficient output losses, while approaches that give less weight to energy-driven price fluctuations—such as core inflation targeting—deliver outcomes more in line with the welfare-maximizing solution.

5.2 Counterfactual Analysis

To better understand the mechanisms shaping the optimal monetary policy response, Figure 8 presents a set of counterfactual experiments in which key estimated frictions are sequentially removed. Starting from the baseline (black dash-dotted line), I first eliminate hand-to-mouth households by setting $\lambda = 0$, yielding a RANK economy shown by the red dashed line. Since liquidity-constrained households are more vulnerable to higher energy costs, their removal dampens the fall in aggregate demand and output. Consequently, the Ramsey planner cuts the policy rate less aggressively.

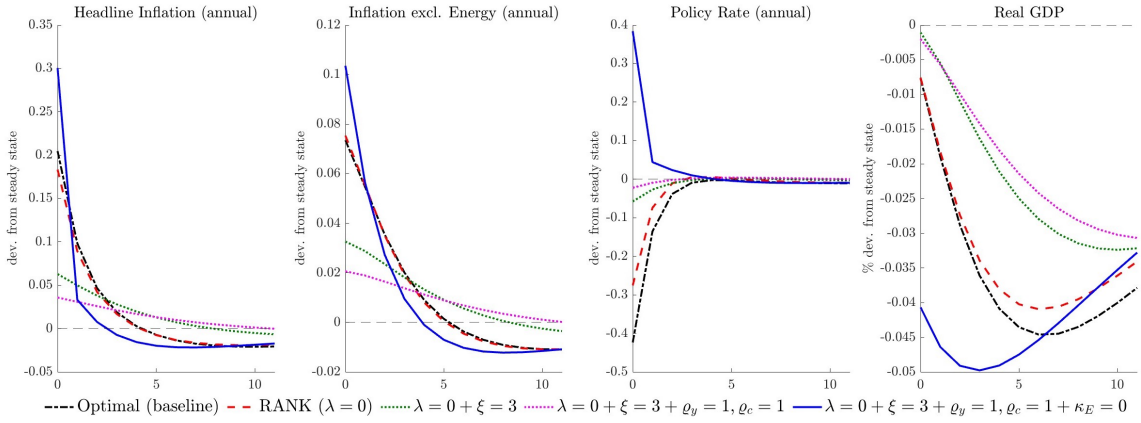

Figure 8: Drivers of the optimal monetary policy response to a carbon price shock

The figure shows a sequence of counterfactuals removing key model features step by step: (i) RANK ($\lambda = 0$); (ii) higher substitutability between green and fossil energy ($\xi = 3$); (iii) Cobb–Douglas production and consumption ($\varrho_y = \varrho_c = 1$); and (iv) no fossil energy adjustment costs ($\kappa_E = 0$).

In the next step, depicted by the green dotted line, I raise the substitutability between

fossil and green energy to $\xi = 3$. This facilitates adjustment in the energy mix, substantially mitigating the rise in production costs and inflation, and further reduces the need for monetary easing. When I additionally allow for Cobb–Douglas substitution between energy and non-energy goods in both production and consumption ($\varrho_c = 1$, $\varrho_y = 1$), the carbon price shock becomes even less distortionary. Firms and households can now substitute away from energy, which strongly mitigates the effects of the shock on inflation and output, as depicted by the pink dotted line. The optimal interest rate response turns nearly flat, but still falls initially.

Finally, setting the fossil energy adjustment cost to zero ($\kappa_E = 0$) allows an instantaneous shift away from fossil inputs. This generates a short-lived but strong surge in energy inflation, which transmits directly to headline and core inflation, as depicted by the blue solid line. At the same time, the fall in aggregate demand is strongly dampened by the parameter settings in the previous steps. The planner therefore raises the policy rate temporarily, resulting in a sharper initial contraction in real GDP. Note that removing the adjustment costs alone does not result in a contractionary monetary policy response, but instead induces the planner to cut the interest rate even stronger initially, as shown in Figure 14 in the Appendix.

Overall, these counterfactuals highlight that the combination of energy rigidities, complementarity, and heterogeneity is crucial for obtaining an optimal easing response to carbon price shocks. Without these features, the model would instead prescribe contractionary monetary policy, which would aggravate the significant decline in aggregate demand observed in the data.

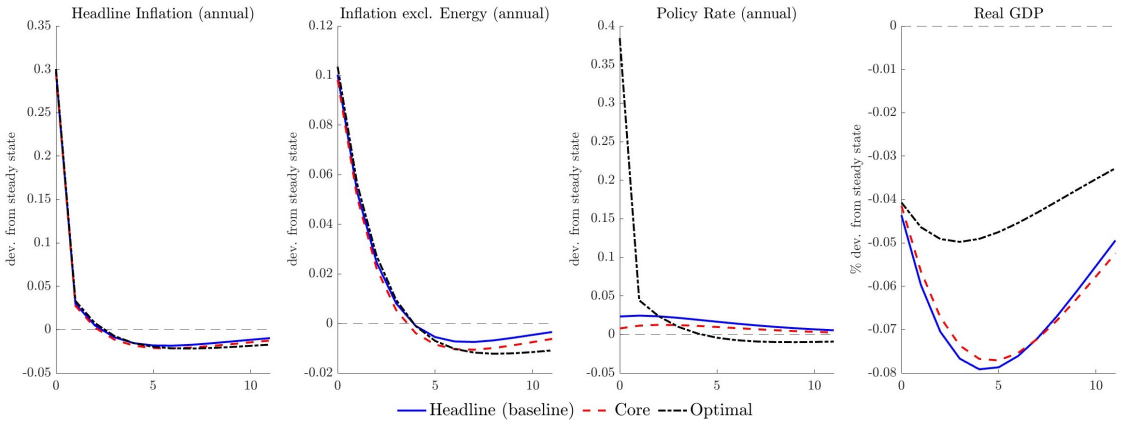

Figure 9: Optimal monetary policy vs. headline inflation stabilization vs. core inflation stabilization with $\lambda = 0 + \xi = 3 + \varrho_y = 1, \varrho_c = 1 + \kappa_E = 0$

Figure 9 compares the optimal policy response with Taylor rules targeting headline and core inflation in a model with $\lambda = 0$, $\xi = 3$, $\varrho_y = 1$, $\varrho_c = 1$, and $\kappa_E = 0$. All other parameters are kept at their calibrated or estimated values. The optimal policy features a sharp initial increase in the nominal interest rate, followed by a gradual normalization,

with the rate slightly declining about one year after the shock. This anticipated easing helps to cushion aggregate demand and limits the contraction in real GDP. The responses of headline and core inflation are almost identical across all three policy regimes, reflecting the dominant role of the exogenous rise in energy prices, which monetary policy cannot directly offset. Compared to the baseline model results in Figure 7, the planner still mitigates the fall in GDP, but not to the extent that it would generate an even stronger inflationary response. Because the demand-side contraction is more muted and the inflationary pressures are stronger under this parameterization, the monetary policy trade-off shifts more toward inflation stabilization relative to the baseline model.

6 Conclusion

In this paper, I develop and estimate a TANK macro-climate model that successfully captures the macroeconomic effects of carbon price shocks in the euro area. Using local projections, I document three key empirical responses to carbon price increases: a gradual decline in emissions, a sharp rise in headline inflation, and a significant drop in economic activity. To replicate these dynamics, I identify four features essential for matching the observed responses: low substitutability between green and fossil energy, fossil energy adjustment costs, strong complementarity between energy and non-energy goods and inputs in consumption and production, and household heterogeneity. The estimated model closely aligns with the data, providing a robust empirical framework for analyzing the macroeconomic implications of carbon pricing. With this empirically grounded framework, I assess the role of monetary policy in shaping macroeconomic outcomes following carbon price shocks. The results show that a welfare-maximizing planner responds to a carbon price shock by lowering the policy rate, prioritizing the stabilization of real activity at the cost of temporarily higher inflation. In the absence of the key frictions identified in the estimation, however, the model would instead prescribe an initially contractionary response, as inflationary pressures dominate when adjustment rigidities and complementarities are removed. A central bank that targets core rather than headline inflation can substantially mitigate the GDP losses following a carbon price shock, thereby approximating the welfare-optimal policy outcome. These findings contribute to the macro-climate modeling literature by providing a framework that captures the complex interaction between carbon pricing and monetary policy. As carbon pricing becomes a central instrument of climate policy, such models are essential for designing effective stabilization strategies in the green transition.

References

Acemoglu, Daron, Philippe Aghion, Leonardo Bursztyn, and David Hemous (2012). "The environment and directed technical change". In: *American economic review* 102.1, pp. 131–166.

Annicchiarico, Barbara and Fabio Di Dio (2015). "Environmental policy and macroeconomic dynamics in a new Keynesian model". In: *Journal of Environmental Economics and Management* 69, pp. 1–21.

Auclert, Adrien, Hugo Monnery, Matthew Rognlie, and Ludwig Straub (2023). *Managing an energy shock: Fiscal and monetary policy*. Tech. rep. National Bureau of Economic Research.

Barrage, Lint (2020). "Optimal dynamic carbon taxes in a climate–economy model with distortionary fiscal policy". In: *The Review of Economic Studies* 87.1, pp. 1–39.

Baumeister, Christiane and James D Hamilton (2019). "Structural interpretation of vector autoregressions with incomplete identification: Revisiting the role of oil supply and demand shocks". In: *American Economic Review* 109.5, pp. 1873–1910.

Benmir, Ghassane, Ivan Jaccard, and Gauthier Vermandel (2020). *Green asset pricing*. Tech. rep. ECB Working Paper No. 2477.

Chan, Jenny, Sebastian Diz, and Derrick Kanngiesser (2024). "Energy prices and household heterogeneity: Monetary policy in a gas-tank". In: *Journal of Monetary Economics* 147, p. 103620.

Christiano, Lawrence J, Martin Eichenbaum, and Charles L Evans (2005). "Nominal rigidities and the dynamic effects of a shock to monetary policy". In: *Journal of political Economy* 113.1, pp. 1–45.

Christiano, Lawrence J, Mathias Trabandt, and Karl Walentin (2010). "DSGE models for monetary policy analysis". In: *Handbook of monetary economics*. Vol. 3. Elsevier, pp. 285–367.

Coenen, Günter, Peter Karadi, Sebastian Schmidt, and Anders Warne (2018). "The New Area-Wide Model II: an extended version of the ECB's micro-founded model for forecasting and policy analysis with a financial sector". In.

Coenen, Günter, Matija Lozej, and Romanos Priftis (2024). "Macroeconomic effects of carbon transition policies: an assessment based on the ECB's New Area-Wide Model with a disaggregated energy sector". In: *European Economic Review* 167, p. 104798.

Del Negro, Marco, Julian Di Giovanni, and Keshav Dogra (2023). "Is the Green Transition Inflationary?" In: *FRB of New York Staff Report* 1053.

Diluiso, Francesca, Barbara Annicchiarico, Matthias Kalkuhl, and Jan C Minx (2021). "Climate actions and macro-financial stability: The role of central banks". In: *Journal of Environmental Economics and Management* 110, p. 102548.

Dossche, Maarten, Jiri Slacalek, and Guido Wolswijk (2021). "Monetary policy and inequality". In: *Economic Bulletin Articles* 2.

Erceg, Christopher, Marcin Kolasa, Jesper Lindé, and Andrea Pescatori (2024). "Can Energy Subsidies Help Slay Inflation?" In.

Gagliardone, Luca and Mark Gertler (2023). "Oil prices, monetary policy and inflation surges". In.

Golosov, Mikhail, John Hassler, Per Krusell, and Aleh Tsyvinski (2014). "Optimal taxes on fossil fuel in general equilibrium". In: *Econometrica* 82.1, pp. 41–88.

Hassler, John, Per Krusell, and Conny Olovsson (2021). "Directed technical change as a response to natural resource scarcity". In: *Journal of Political Economy* 129.11, pp. 3039–3072.

Hassler, John, Per Krusell, Conny Olovsson, and Michael Reiter (2020). "On the effectiveness of climate policies". In: *IIES WP* 53, p. 54.

Heutel, Garth (2012). "How should environmental policy respond to business cycles? Optimal policy under persistent productivity shocks". In: *Review of Economic Dynamics* 15.2, pp. 244–264.

Känzig, Diego R (2021). "The macroeconomic effects of oil supply news: Evidence from OPEC announcements". In: *American Economic Review* 111.4, pp. 1092–1125.

— (2023). *The unequal economic consequences of carbon pricing*. Tech. rep. National Bureau of Economic Research.

Konradt, Maximilian and Beatrice Weder di Mauro (2023). "Carbon taxation and greenflation: Evidence from europe and canada". In: *Journal of the European Economic Association*, jvad020.

Metcalf, Gilbert E and James H Stock (2023). "The macroeconomic impact of Europe's carbon taxes". In: *American Economic Journal: Macroeconomics* 15.3, pp. 265–286.

Montiel Olea, José Luis and Mikkel Plagborg-Møller (2021). "Local projection inference is simpler and more robust than you think". In: *Econometrica* 89.4, pp. 1789–1823.

Nakov, Anton and Carlos Thomas (2023). "Climate-conscious monetary policy". In.

Nordhaus, William (2008). *A question of balance: Weighing the options on global warming policies*. Yale University Press.

Olovsson, Conny and David Vestin (2023). *Greenflation?* Sveriges Riksbank.

Papageorgiou, Chris, Marianne Saam, and Patrick Schulte (2017). "Substitution between clean and dirty energy inputs: A macroeconomic perspective". In: *Review of Economics and Statistics* 99.2, pp. 281–290.

Quilis, Enrique M. (2024). *Temporal Disaggregation*. Accessed: 30 Oct. 2024. URL: `https://de.mathworks.com/matlabcentral/fileexchange/69800-temporal-disaggregation`.

Sahuc, Jean-Guillaume, Frank Smets, and Gauthier Vermandel (2025). "The New Keynesian Climate Model". In.

Schmitt-Grohé, Stephanie and Martin Uribe (2004). *Optimal operational monetary policy in the Christiano-Eichenbaum-Evans model of the US business cycle*.

Schnabel, Isabel (2022). *A new age of energy inflation: climateflation, fossilflation and greenflation*. Speech by Isabel Schnabel, Member of the Executive Board of the ECB, at a panel on "Monetary Policy and Climate Change" at The ECB and its Watchers XXII Conference. URL: https://www.ecb.europa.eu/press/key/date/2022/html/ecb.sp220317_2~dbb3582f0a.en.html.

Wu, Jing Cynthia and Fan Dora Xia (2020). "Negative interest rate policy and the yield curve". In: *Journal of Applied Econometrics* 35.6, pp. 653–672.

A Model details

This appendix presents the full set of equilibrium conditions. The model is described by a total of 63 equations and 63 endogenous variables $\{c_t, c_{t,R}, c_{t,H}, c^E_{t,R}, c^E_{t,H}, c^X_{t,R}, c^X_{t,H}, \lambda_t, r_t, \pi_t, \pi^R_t, \pi^H_t, \pi^X_t, \pi^E_t, r^{k,Y}_t, r^{k,B}_t, r^{k,G}_t, q^Y_t, q^G_t, q^B_t, u^B_t, u^Y_t, u^G_t, i_t, i^Y_t, i^G_t, i^B_t, k^Y_t, k^G_t, k^B_t, h_{t,R}, h_{t,H}, h^Y_t, h^G_t, h^B_t, e_t, e^Y_t, e^G_t, e^B_t, p_t, p_{t,R}, p_{t,H}, p^E_t, p^G_t, p^B_t, w_t, w_{t,R}, w^*_t, p^{X*}_t, K_t, F_t, d_t, K^W_t, F^W_t, y_t, mc_t, gdp_t, S_t, A^Y_t, A^G_t, A^B_t, \Gamma_t, \Gamma'_t\}$ and an exogenous process for τ_t.

Households:

$$\lambda_t p^R_t = \frac{1}{c_{t,R} - bc_{t-1,R}} - \beta b \frac{1}{c_{t+1,R} - bc_{t,R}} \tag{A.1}$$

$$1 = \beta \mathbb{E}_t \frac{\lambda_{t+1}}{\lambda_t} \frac{r_t}{\pi^X_{t+1}} \tag{A.2}$$

$$q^Y_t = \beta \mathbb{E}_t \frac{\lambda_{t+1}}{\lambda_t} (r^{k,Y}_{t+1} u^Y_{t+1} - a(u^Y_t) + (1-\delta) q^Y_{t+1}) \tag{A.3}$$

$$q^G_t = \beta \mathbb{E}_t \frac{\lambda_{t+1}}{\lambda_t} (r^{k,G}_{t+1} u^G_{t+1} - a(u^G_t) + (1-\delta) q^G_{t+1}) \tag{A.4}$$

$$q^B_t = \beta \mathbb{E}_t \frac{\lambda_{t+1}}{\lambda_t} (r^{k,B}_{t+1} u^B_{t+1} - a(u^B_t) + (1-\delta) q^B_{t+1}) \tag{A.5}$$

$$r^{k,Y}_t = a'(u^Y_t) \tag{A.6}$$

$$r^{k,G}_t = a'(u^G_t) \tag{A.7}$$

$$r^{k,B}_t = a'(u^B_t) \tag{A.8}$$

$$1 = q^Y_t \left[1 - \frac{\kappa_I}{2}\left(\frac{i^Y_t}{i^Y_{t-1}} - 1\right)^2 - \kappa_I \left(\frac{i^Y_t}{i^Y_{t-1}} - 1\right)\frac{i^Y_t}{i^Y_{t-1}}\right] + \beta q^Y_{t+1}\left[\frac{\lambda_{t+1}}{\lambda_t}\kappa_I \left(\frac{i^Y_{t+1}}{i^Y_t} - 1\right)\left(\frac{i^Y_{t+1}}{i^Y_t}\right)^2\right] \tag{A.9}$$

$$1 = q^Y_t \left[1 - \frac{\kappa_I}{2}\left(\frac{i^G_t}{i^G_{t-1}} - 1\right)^2 - \kappa_I \left(\frac{i^G_t}{i^G_{t-1}} - 1\right)\frac{i^G_t}{i^G_{t-1}}\right] + \beta q^G_{t+1}\left[\frac{\lambda_{t+1}}{\lambda_t}\kappa_I \left(\frac{i^G_{t+1}}{i^G_t} - 1\right)\left(\frac{i^G_{t+1}}{i^G_t}\right)^2\right] \tag{A.10}$$

$$1 = q^B_t \left[1 - \frac{\kappa_I}{2}\left(\frac{i^B_t}{i^B_{t-1}} - 1\right)^2 - \kappa_I \left(\frac{i^B_t}{i^B_{t-1}} - 1\right)\frac{i^B_t}{i^B_{t-1}}\right] + \beta q^B_{t+1}\left[\frac{\lambda_{t+1}}{\lambda_t}\kappa_I \left(\frac{i^B_{t+1}}{i^B_t} - 1\right)\left(\frac{i^B_{t+1}}{i^B_t}\right)^2\right] \tag{A.11}$$

$$k^Y_t = (1-\delta)k^Y_{t-1} + \left(1 - \frac{\kappa_I}{2}\left(\frac{i^Y_t}{i^Y_{t-1}} - 1\right)^2\right) i^Y_t \tag{A.12}$$

$$k^G_t = (1-\delta)k^G_{t-1} + \left(1 - \frac{\kappa_I}{2}\left(\frac{i^G_t}{i^G_{t-1}} - 1\right)^2\right) i^G_t \tag{A.13}$$

$$k^B_t = (1-\delta)k^B_{t-1} + \left(1 - \frac{\kappa_I}{2}\left(\frac{i^B_t}{i^B_{t-1}} - 1\right)^2\right) i^B_t \tag{A.14}$$

$$p_t^H c_{t,H} = w_t h_{t,H} \tag{A.15}$$

$$h_{t,H} = h_{t,R} \tag{A.16}$$

$$p_t^R = \left(\gamma_{c,R}(p_t^E)^{1-\varrho_c} + (1-\gamma_{c,R})\right)^{\frac{1}{1-\varrho}} \tag{A.17}$$

$$p_t^H = \left(\gamma_{c,H}(p_t^E)^{1-\varrho_c} + (1-\gamma_{c,H})\right)^{\frac{1}{1-\varrho}} \tag{A.18}$$

$$c_{t,R}^E = \gamma_c \left(\frac{p_t^E}{p_t^R}\right)^{-\varrho_c} c_{t,R} \tag{A.19}$$

$$c_{t,R}^X = (1-\gamma_{c,R}) \left(\frac{1}{p_t^R}\right)^{-\varrho_c} c_{t,R} \tag{A.20}$$

$$c_{t,H}^E = \gamma_{c,H} \left(\frac{p_t^E}{p_t^H}\right)^{-\varrho_c} c_{t,H} \tag{A.21}$$

$$c_{t,H}^X = (1-\gamma_{c,H}) \left(\frac{1}{p_t^H}\right)^{-\varrho_c} c_{t,H} \tag{A.22}$$

Wage setting:

$$w_{t,R} = \frac{w_t}{p_{t,R}} \tag{A.23}$$

$$w_{t,R} = \left(\theta_W w_{t-1,R}^{1-\varepsilon_W} + (1-\theta_W)(w_{t,R}^*)^{1-\varepsilon_W}\right)^{\frac{1}{1-\varepsilon_w}} \tag{A.24}$$

$$(w_{t,R}^*)^{1+\phi\varepsilon_W} = \frac{\varepsilon_W}{\varepsilon_W - 1} \frac{K_t^W}{F_t^W} \tag{A.25}$$

$$K_t^W = (w_{t,R}^{\varepsilon_W} h_{t,R})^{1+\phi} + \theta_W \beta (\pi_{t+1}^R)^{(1+\phi)\varepsilon_W} K_{t+1}^W \tag{A.26}$$

$$F_t^W = w_{t,R}^{\varepsilon_W} h_{t,R} \lambda_t p_{t,R} + \theta_W \beta (\pi_{t+1}^R)^{(1+\phi)\varepsilon_W - 1} F_{t+1}^W \tag{A.27}$$

Firms:

$$y_t d_t = \left[(1-\gamma_Y)^{\frac{1}{\varrho_Y}} \left((A_t^Y u_t^Y k_{t-1}^Y)^\alpha (h_t^Y)^{1-\alpha}\right)^{\frac{\varrho_Y - 1}{\varrho_Y}} + (\gamma_Y)^{\frac{1}{\varrho_Y}} (e_t^Y)^{\frac{\varrho_Y - 1}{\varrho_Y}} \right]^{\frac{\varrho_Y}{\varrho_Y - 1}} \tag{A.28}$$

$$w_t = mc_t \left((1-\gamma_Y) y_t d_t\right)^{\frac{1}{\varrho_Y}} \left(A_t^Y (u_t^Y k_{t-1}^Y)^\alpha (h_t^Y)^{1-\alpha}\right)^{\frac{\varrho_Y - 1}{\varrho_Y}} (1-\alpha) \frac{1}{h_t^Y} \tag{A.29}$$

$$r_t^{k,Y} = mc_t \left((1-\gamma_Y) y_t d_t\right)^{\frac{1}{\varrho_Y}} \left((A_t^Y u_t^Y k_{t-1}^Y)^\alpha (h_t^Y)^{1-\alpha}\right)^{\frac{\varrho_Y - 1}{\varrho_Y}} \alpha \frac{1}{u_t^Y k_{t-1}^Y} \tag{A.30}$$

$$e_t^Y = \left(\frac{p_t^E}{mc_t}\right)^{-\varrho_Y} \gamma_Y y_t d_t \tag{A.31}$$

Price setting:

$$1 = \left(\theta_P \left(\frac{\pi_t^X}{\pi} \right)^{\varepsilon - 1} + (1 - \theta_P)(p_t^{X*})^{1-\varepsilon} \right)^{\frac{1}{1-\varepsilon}} \tag{A.32}$$

$$p_t^{X*} = \frac{\varepsilon}{\varepsilon - 1} \frac{K_t}{F_t} \tag{A.33}$$

$$K_t = y_t m c_t \lambda_t + \theta_P \beta \left(\frac{\pi_{t+1}^X}{\pi} \right)^{\varepsilon_W} K_{t+1} \tag{A.34}$$

$$F_t = y_t \lambda_t + \theta_P \beta \left(\frac{\pi_{t+1}^X}{\pi} \right)^{\varepsilon - 1} F_{t+1} \tag{A.35}$$

$$d_t = (1 - \theta_P) \left(p_t^{X*} \right)^{-\varepsilon} + \theta_P \left(\frac{\pi_t^X}{\pi} \right)^{\varepsilon} d_{t-1} \tag{A.36}$$

Energy firms:

$$e_t = \left((1 - \zeta)^{\frac{1}{\xi}} (e_t^G)^{\frac{\xi - 1}{\xi}} + \zeta^{\frac{1}{\xi}} (e_t^F (1 - \Gamma_t))^{\frac{\xi - 1}{\xi}} \right)^{\frac{\xi}{\xi - 1}} \tag{A.37}$$

$$e_t^F = \zeta \left(\frac{p_t^B (1 + \tau_t)}{p_t^E (1 - \Gamma_t - \Gamma_t' e_t^F)} \right)^{-\xi} \frac{e_t}{1 - \Gamma_t} \tag{A.38}$$

$$e_t^G = (1 - \zeta) \left(\frac{p_t^G}{p_t^E} \right)^{-\xi} e_t \tag{A.39}$$

$$\Gamma_t = \frac{\kappa_E}{2} \left(\frac{e_t^F}{e_{t-1}^F} - 1 \right)^2 \tag{A.40}$$

$$\Gamma_t' = \kappa_E \frac{1}{e_{t-1}^F} \left(\frac{e_t^F}{e_{t-1}^F} - 1 \right) \tag{A.41}$$

$$e_t^B = A_t^B (u_t^B k_{t-1}^B)^{\alpha_E} (h_t^B)^{1 - \alpha_E} \tag{A.42}$$

$$e_t^G = A_t^G (u_t^G k_{t-1}^G)^{\alpha_E} (h_t^G)^{1 - \alpha_E} \tag{A.43}$$

$$(1 - \alpha_E) p_t^B e_t^B = w_t h_t^B \tag{A.44}$$

$$(1 - \alpha_E) p_t^G e_t^G = w_t h_t^G \tag{A.45}$$

$$\alpha_E p_t^B e_t^B = r_t^{k,B} u_t^B k_{t-1}^B \tag{A.46}$$

$$\alpha_E p_t^G e_t^G = r_t^{k,G} u_t^G k_{t-1}^G \tag{A.47}$$

Climate change:

$$S_t = (1 - \delta_S) S_{t-1} + (m_t + m^{row}), \tag{A.48}$$

$$A_t^Y = a_t^Y e^{-\psi S_t} \tag{A.49}$$

$$A_t^B = a_t^B e^{-\psi S_t} \tag{A.50}$$

$$A_t^G = a_t^G e^{-\psi S_t} \tag{A.51}$$

Aggregation, Market clearing and policy:

$$\frac{r_t}{r} = \left(\frac{r_{t-1}}{r}\right)^{\rho_r} \left[\left(\frac{\pi_t}{\pi}\right)^{\phi_\pi} \left(\frac{y_t}{y}\right)^{\phi_y}\right]^{(1-\rho_r)}, \tag{A.52}$$

$$(1-\lambda)h_{t,R} + \lambda h_{t,H} = h_t^Y + h_t^B + h_t^G \tag{A.53}$$

$$i_t = i_t^Y + i_t^B + i_t^G \tag{A.54}$$

$$e_t = e_t^Y + \lambda c_{t,H}^E + +(1-\lambda)c_{t,R}^E \tag{A.55}$$

$$p_t c_t = \lambda p_{t,H} c_{t,H} + (1-\lambda) p_{t,R} c_{t,R} \tag{A.56}$$

$$p_t = \lambda p_{t,H} + (1-\lambda) p_{t,R} \tag{A.57}$$

$$y_t = c_t^X + i_t + g + \sum_j a(u_t^j) k_{t-1}^j, \quad j \in \{Y, B, G\} \tag{A.58}$$

$$gdp_t = p_t c_t + i_t + g \tag{A.59}$$

$$\pi_t = \frac{p_t}{p_{t-1}} \pi_t^X \tag{A.60}$$

$$\pi_t^E = \frac{p_t^E}{p_{t-1}^E} \pi_t^X \tag{A.61}$$

$$\pi_t^R = \frac{p_t^R}{p_{t-1}^R} \pi_t^X \tag{A.62}$$

$$\pi_t^H = \frac{p_t^H}{p_{t-1}^H} \pi_t^X \tag{A.63}$$

Exogenous processes:

$$\log(\tau_t) = (1-\rho_\tau)\log(\overline{\tau}) + \rho_\tau \log(\tau_{t-1}) + \epsilon_t^\tau \tag{A.64}$$

B Additional Figures

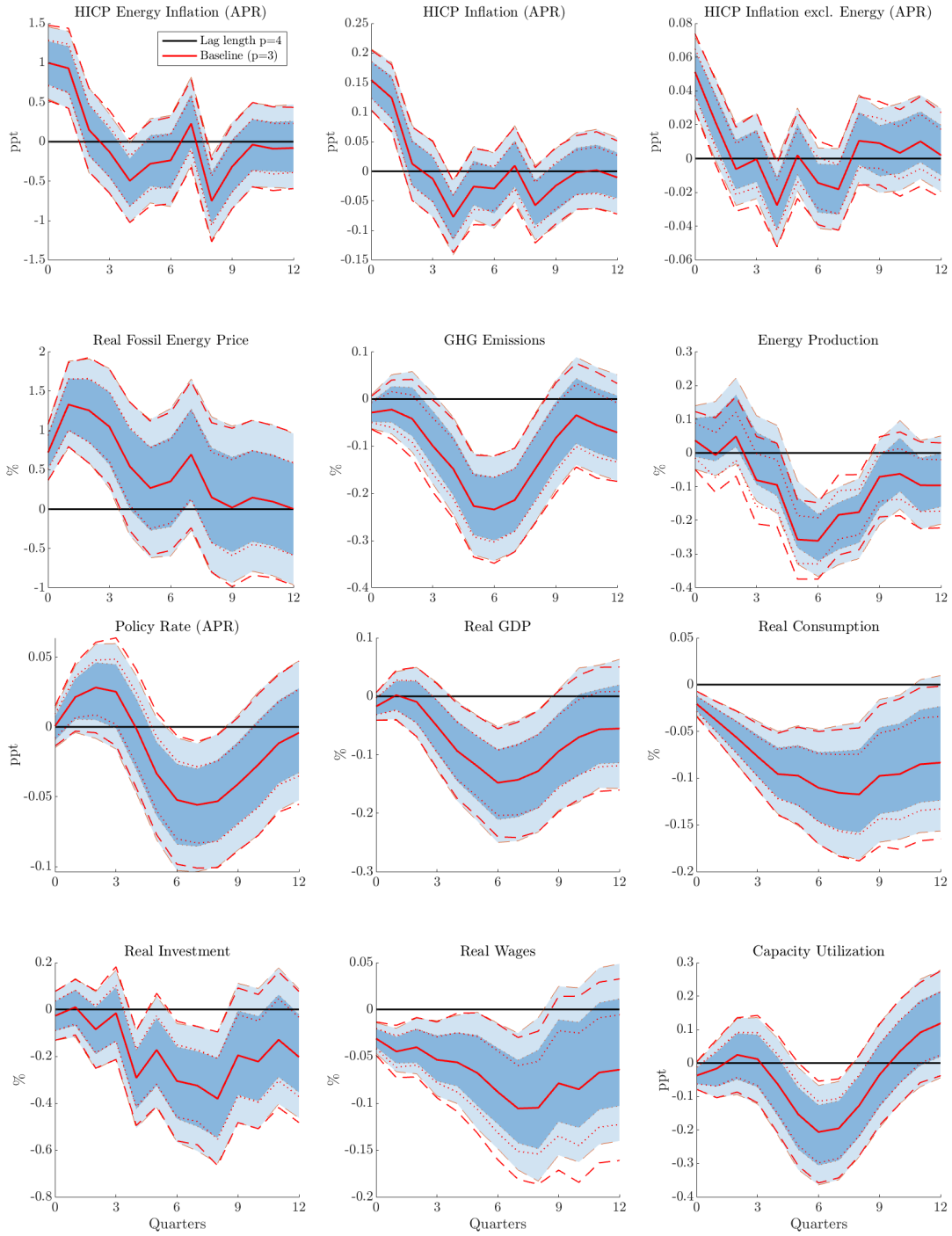

Figure 10: Impulse responses - Alternative lag length

The solid line is the point estimate, the dark and light shaded areas are 68 and 90 % confidence bands. The baseline point estimate is depicted by the red line. The dotted and dashed red lines are the baseline 68 and 90 % confidence bands.
The shock is normalized to increase annual energy inflation by 1 ppt.

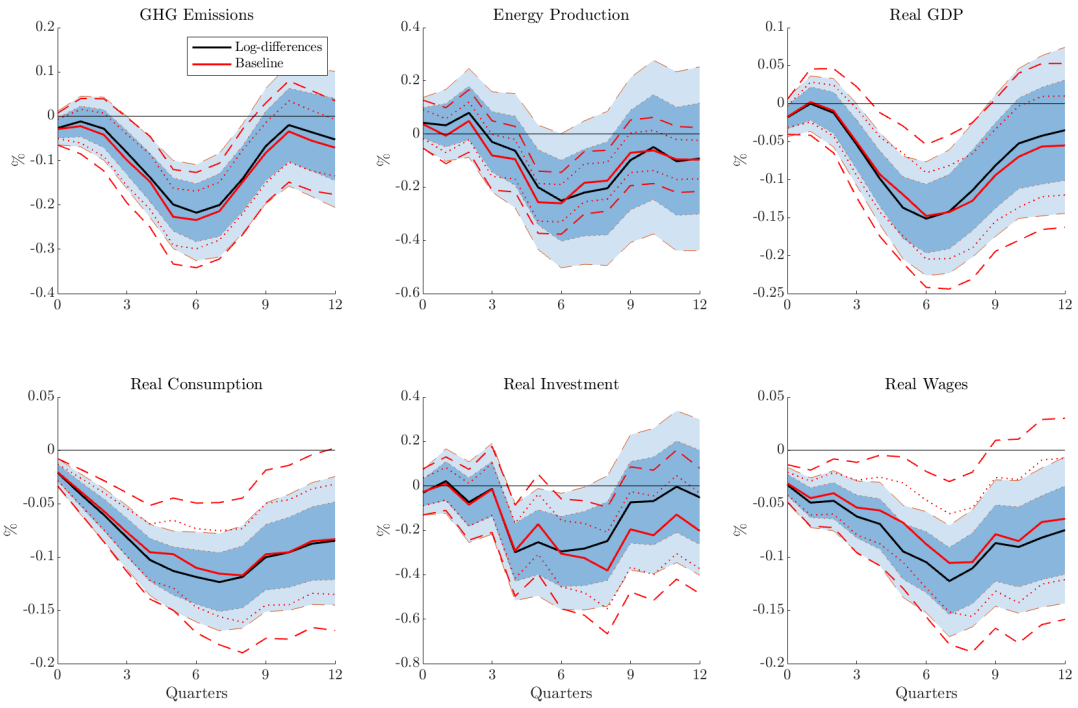

Figure 11: Impulse responses - Estimation based on log-differnces

The solid line is the point estimate, the dark and light shaded areas are 68 and 90 % confidence bands. The baseline point estimate is depicted by the red line. The dotted and dashed red lines are the baseline 68 and 90 % confidence bands.
The shock is normalized to increase annual energy inflation by 1 ppt.

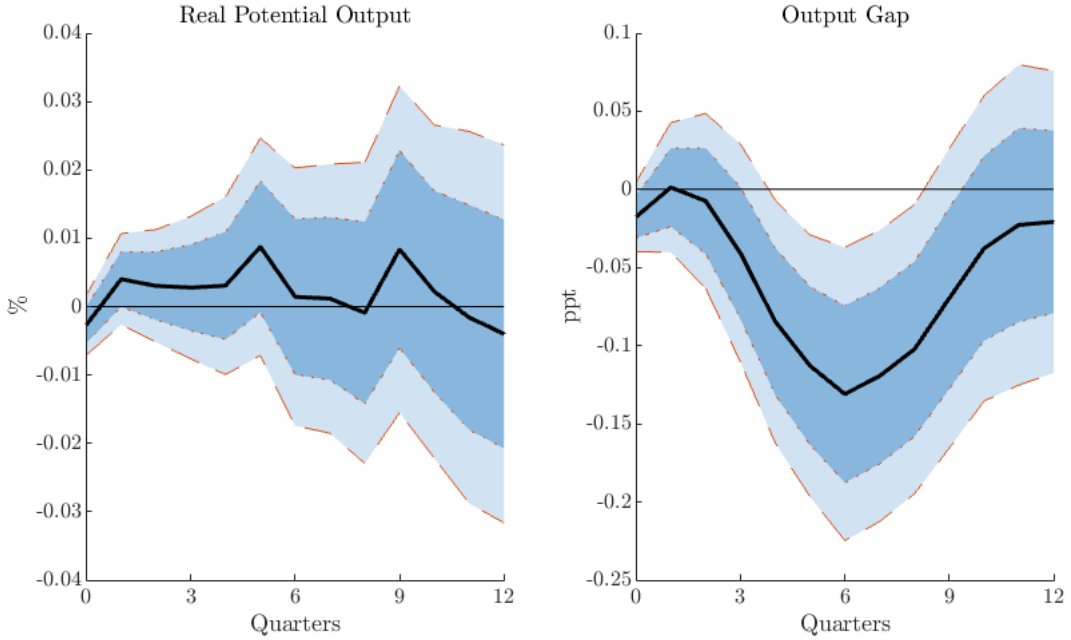

Figure 12: Impulse responses of potential output and the output gap

The solid line is the point estimate, the dark and light shaded areas are 68 and 90 % confidence bands.
The shock is normalized to increase annual energy inflation by 1 ppt.

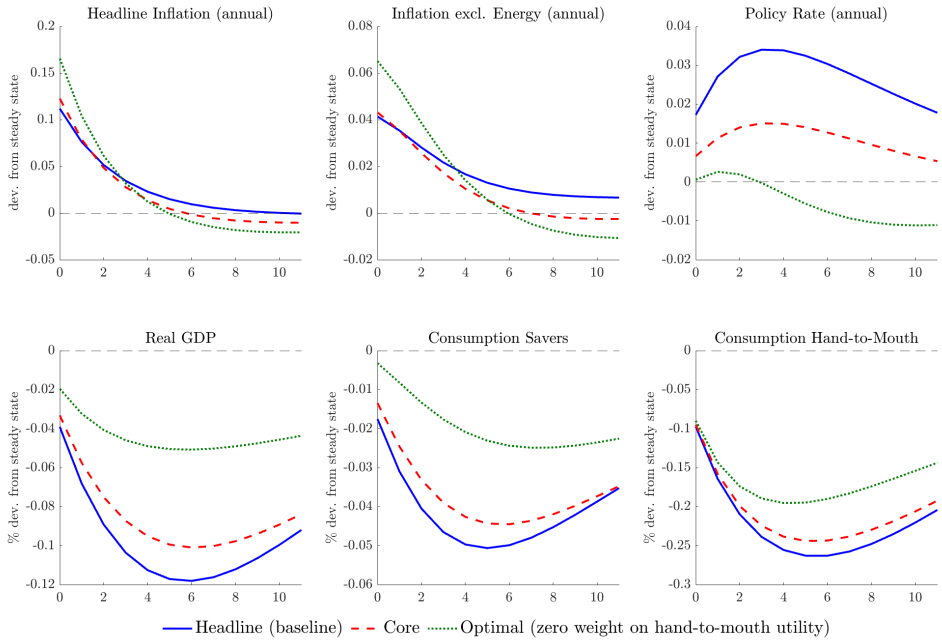

Figure 13: Impulse responses to a carbon price shock: Optimal monetary policy vs. headline inflation stabilization vs. core inflation stabilization

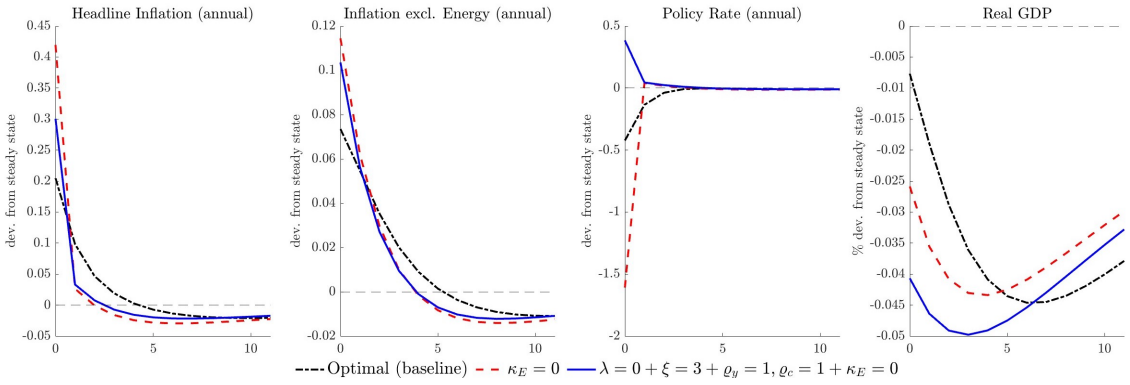

Figure 14: Fossil energy adjustment cost as driver of the optimal monetary policy response